

Report No. BMI-1436

UC-25 Metallurgy and Ceramics  
(TID-4500, 15th Ed.)

Contract No. W-7405-eng-92

FURTHER DEVELOPMENT OF GAS-PRESSURE BONDING  
OF ZIRCALOY-CLAD FLAT-PLATE URANIUM  
DIOXIDE FUEL ELEMENTS

by

Stan J. Paprocki  
Edwin S. Hodge  
Edwin H. Layer  
Edwin G. Wintucky  
Paul J. Gripshover  
Donald C. Carmichael

May 11, 1960

BATTELLE MEMORIAL INSTITUTE  
505 King Avenue  
Columbus 1, Ohio

## **DISCLAIMER**

**This report was prepared as an account of work sponsored by an agency of the United States Government. Neither the United States Government nor any agency Thereof, nor any of their employees, makes any warranty, express or implied, or assumes any legal liability or responsibility for the accuracy, completeness, or usefulness of any information, apparatus, product, or process disclosed, or represents that its use would not infringe privately owned rights. Reference herein to any specific commercial product, process, or service by trade name, trademark, manufacturer, or otherwise does not necessarily constitute or imply its endorsement, recommendation, or favoring by the United States Government or any agency thereof. The views and opinions of authors expressed herein do not necessarily state or reflect those of the United States Government or any agency thereof.**

## **DISCLAIMER**

**Portions of this document may be illegible in electronic image products. Images are produced from the best available original document.**

## TABLE OF CONTENTS

	<u>Page</u>
ABSTRACT . . . . .	1
INTRODUCTION . . . . .	1
COATING OF URANIUM DIOXIDE CORES . . . . .	2
Development of the Vacuum-Evaporation Process for Coating Uranium Dioxide Cores With Chromium . . . . .	3
Materials and Equipment . . . . .	4
Coating Procedure . . . . .	7
Determination of the Thickness of the Coatings . . . . .	8
Tests for Adherency of the Coatings . . . . .	8
Results of the Preliminary Evaluation of the Coatings . . . . .	8
Development of the Pyrolytic Process for Coating Uranium Dioxide Cores With Crystalline Carbon . . . . .	12
Materials and Equipment . . . . .	12
Sandblasting of the Cores Prior to Coating . . . . .	12
Coating Procedure . . . . .	13
Techniques for Measuring the Thickness of the Coatings . . . . .	13
Tests for Adherency of the Coatings . . . . .	14
Results of the Preliminary Evaluation of the Coatings . . . . .	14
BOND-TEST RESULTS WITH PYROLYTIC CARBON, VAPOR-DEPOSITED CHROMIUM, AND GRAPHITE COATINGS . . . . .	16
Metallographic Examination . . . . .	20
Corrosion and Intercompartmental-Leakage Testing . . . . .	29
Results of Burst Tests . . . . .	31
Results of Chemical Analyses of the Cladding . . . . .	33
Study of Flow of Cladding During Gas-Pressure Bonding Into Void Spaces in Picture Frames of Fuel Elements . . . . .	34
Results of Visual Examination . . . . .	35
Results of Metallographic Examination of Flow . . . . .	42
Cleaning and Assembly of Specimens for Bonding . . . . .	50
CONCLUSIONS . . . . .	56
ACKNOWLEDGMENT . . . . .	57
REFERENCES . . . . .	57

FURTHER DEVELOPMENT OF GAS-PRESSURE BONDING OF ZIRCALOY-CLAD  
FLAT-PLATE URANIUM DIOXIDE FUEL ELEMENTS

by

Stan J. Paprocki, Edwin S. Hodge, Edwin H. Layer, Edwin G. Wintucky,  
Paul J. Gripshover, and Donald C. Carmichael

*The effects of core barrier coatings, void spaces, and surface-cleaning techniques on the quality of Zircaloy-clad flat-plate  $UO_2$  fuel elements prepared by gas-pressure bonding were investigated in a continuation of the development program reported in BMI-1374.*

*Techniques were developed for the application of barrier layers of chromium by a vapor-deposition process and of crystalline carbon by a pyrolytic process. These coatings, together with a graphite coating developed previously, were then evaluated in pressure-bonded fuel elements for their effectiveness in preventing core-to-cladding reaction and for their general production feasibility. Crystalline carbon coatings 15 to 40  $\mu$  in. thick and chromium coatings 25 to 40  $\mu$  in. thick were determined to be satisfactory.*

*In the study of the flow of cladding-plate material into void spaces in the picture-frame assembly, it was established that excessive flow, and consequent thinning of the cladding, can be minimized by individually compartmentalizing the cores with Zircaloy ribs. This design also results in maximum restriction of the effects of a cladding failure in service. Quantitative data on the maximum amount of void space resulting from manufacturing tolerances or from chipped fuel cores that is tolerable in elements of this design were obtained.*

*Studies of surface-cleaning techniques were limited to refinement of procedures established previously. It was found that a final multistep rinsing cycle resulted in bonds consistently free of evidence of contamination.*

INTRODUCTION

Previous studies(1, 2) of the gas-pressure-bonding process for producing plate-type uranium dioxide fuel elements clad with Zircaloy(3-5) showed that this method has considerable promise. The general techniques for preparing fuel elements of this type were developed in this earlier work. It was found that satisfactory fuel elements could be prepared by this method, but that there were certain difficulties which needed to be corrected before the process could be considered suitable for the routine production of plate-type fuel elements:

- (1) At bonding temperatures, a reaction occurs between  $UO_2$  and Zircaloy which results in poor corrosion behavior of the fuel elements.(2, 6) It is essential to coat the  $UO_2$  with some material which prevents this reaction and which itself does not detrimentally with the Zircaloy. It was found in the

earlier work that, under some conditions, sprayed graphite coatings prevented the reaction satisfactorily, but the results obtained with sprayed graphite coats were inconsistent. Furthermore, it was shown that the graphite can be rubbed from the cores and contaminate the Zircaloy surfaces to such an extent that satisfactory Zircaloy-to-Zircaloy bonds are not obtained. For these reasons, improved barrier coating materials were required. In the present study, two types of barrier coats were investigated: coatings of pyrolytic carbon formed by the cracking of hydrocarbon gases at elevated temperatures and coatings of chromium deposited by evaporation. Previous work had shown the efficacy of the chromium coats prepared by electroplating, but electroplating was considered an uneconomical method and was not investigated further.

- (2) Because of the dimensional tolerances of the components, some void spaces in the picture-frame assembly will exist initially in the bonding cycle. These voids must be filled by deformation of the cladding components of the fuel element. This sometimes leads to extreme deformation and even to rupture of the cladding. An objective of the present program was the determination of the conditions under which excessive deformation occurs and the development of practical methods to prevent it. In this work, the effects of dimensional tolerances and of core chipping were studied and related to the design of the fuel element.
- (3) Occasional difficulties arose in the previous studies in producing satisfactory Zircaloy-to-Zircaloy bonds that could not be attributed to contamination by the barrier coating. Further investigation of the surface cleaning of Zircaloy prior to bonding was undertaken in the present program in an attempt to eliminate such inconsistencies.

#### COATING OF URANIUM DIOXIDE CORES

Coatings of pyrolytic carbon, vacuum-evaporated chromium, and sprayed graphite were applied to uranium dioxide cores to evaluate their effectiveness in preventing reaction and their effect, if any, on the Zircaloy-to-Zircaloy bonding in pressure-bonded fuel elements. Satisfactory techniques for coating uranium dioxide cores with crystalline carbon by a pyrolytic process and with chromium by vacuum evaporation were developed. These processes will be discussed in detail in a later section. The application of a chromium coating by reduction of a dipped chromous iodide film was also studied in this program. In the process developed, the cores were dipped into a bath of liquid chromous iodide contained in a reaction chamber and then removed from the bath into an atmosphere of hydrogen, which reduced the dipped films to chromium. Since this process did not appear to be as economical or as fully developed for coating as vacuum evaporation of chromium, it was not used to prepare cores for evaluation in pressure-bonded elements.

Graphite coatings were sprayed onto the cores according to procedures developed in the previous program.<sup>(2)</sup> Aquadag, a suspension of graphite in water, was sprayed

onto the  $UO_2$  cores which were preheated to approximately 150 F. The feed was adjusted so that 5 to 6 mg of graphite was applied per in.<sup>2</sup> of core surface by making three to five passes per side with the spray gun. The coated cores were outgassed at 750 F in vacuum to remove all volatiles from the graphite coatings and were then buffed to a high luster by rubbing them firmly with a soft cloth, which removed approximately 0.5 mg of the graphite coating per in.<sup>2</sup> of core surface. The buffing treatment has been found to decrease the amount of dusting and flaking of the coatings that results in contamination of bonds; however, it was difficult to assemble  $UO_2$  cores into the Zircaloy receptacles without producing some contamination of the bonding surfaces. As a result, it was the intent of this study to develop a more suitable coating than the sprayed and buffed graphite.

#### Development of the Vacuum-Evaporation Process for Coating Uranium Dioxide Cores With Chromium

The application of thin coatings of chromium onto uranium dioxide cores by the process of vacuum evaporation, or vacuum metallizing, was studied to attempt to develop a coating which would be a satisfactory barrier to core-to-cladding reaction during gas-pressure bonding and which would not have an adverse effect on the quality of the bonding obtained between the Zircaloy components of the fuel elements. In this process, pure chromium is evaporated in vacuo from an electrically heated molybdenum or tungsten boat, and condenses on the surfaces of the cooler, suitably positioned uranium dioxide cores. This coating technique was investigated because experiments in a previous program<sup>(2)</sup> using electroplated chromium coatings on the  $UO_2$  cores had indicated that chromium was a suitable barrier material. It was anticipated that vacuum evaporation, which is used commercially for inexpensively coating electronic components and novelties with very thin metal films, would be more economical than electroplating if chromium coatings of sufficient thickness could be applied economically. Commercial applications of this process have normally required only very thin films, of the order of 1  $\mu$ in. thick, which were not expected to be a sufficient barrier in these fuel elements. The electroplated coatings which had been studied were approximately 500  $\mu$ in. thick, and since it would probably not be practical to vacuum evaporate coating to this thickness, it was necessary to determine if thinner evaporated coatings would be satisfactory barriers to core-to-cladding reaction. It was expected that the pure chromium coatings would not, by their nature, have any deleterious effect on the Zircaloy-to-Zircaloy bonding in the pressure-bonded fuel elements.

In the investigation of the vacuum-evaporation process, therefore, it was necessary to develop procedures for applying comparatively thick coatings of chromium which were adherent and nonporous directly onto the uranium dioxide cores. A method for rotating the cores during the coating process had to be developed, since vacuum evaporation results in straight-line deposition of the coating material onto those surfaces of the pieces to be coated which are facing the source of the evaporating metal. It was also desired to determine from gas-pressure-bonding studies the minimum thickness of chromium which would satisfactorily minimize core-to-cladding reaction and to establish that the coating had no effect on the Zircaloy-to-Zircaloy bonding in pressure-bonded fuel elements. In this study, the coatings of chromium applied to

$\text{UO}_2$  cores under various conditions were subjected to preliminary evaluation to determine their thickness and adherency. The results are discussed in this section of the report. The conditions which yielded coatings that were satisfactory based on the preliminary evaluations were employed to apply coatings in several thickness ranges to a large number of cores which were then gas-pressure bonded in fuel elements. The coatings were then evaluated on the basis of their behavior in the bonded elements.

#### Materials and Equipment

An 18-in. bell-jar vacuum chamber with a forepump and an oil-diffusion pump capable of attaining an ultimate pressure of  $1 \times 10^{-5}$  mm of mercury in the chamber was used in the vacuum-evaporation process and is shown in Figure 1.

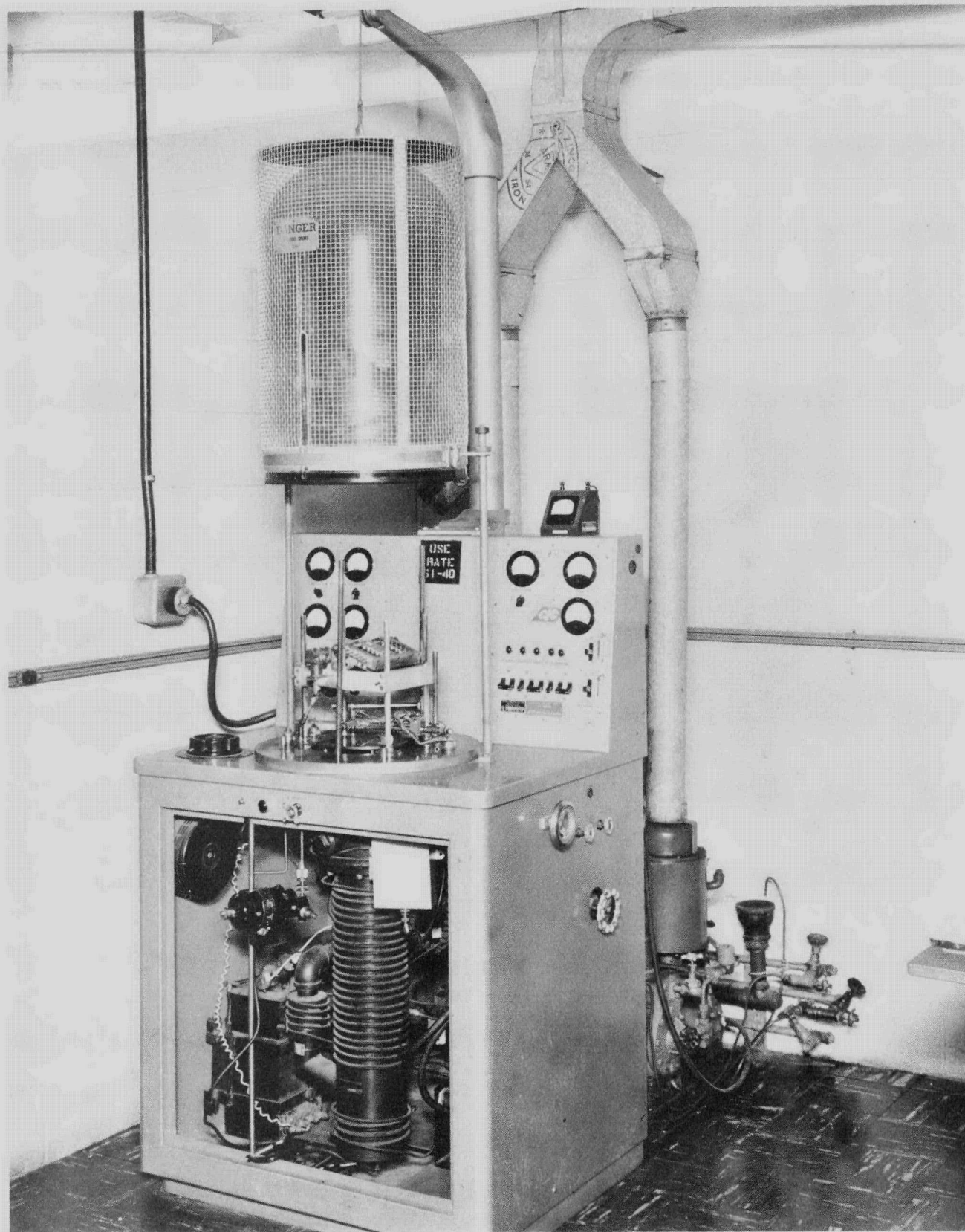
The source material for evaporation was pure chromium purchased from the Chromalloy Corporation. Less than 28 ppm of gaseous and metallic impurities was detected by the vendor's chemical analysis of the chromium. Because chromium tends to sublime rather than melt, an important factor in the evaporation of chromium is the thermal contact between it and the boat. Adequate thermal contact was attained by crushing the chromium into fine pieces 1 mm or less in diameter.

Molybdenum was usually employed in this program for the filament heater, or boat, for the evaporation of chromium. The molybdenum was available in sheet form which was malleable at room temperature and could be cut with shears; therefore, boats of almost any desired shape and size were easily formed. A molybdenum boat normally lasted for three to six evaporation before failure occurred due to alloying with the chromium.

The dimensions of the molybdenum boats used were varied. The most satisfactory ones were cut from 0.010-in.-thick sheet and were about 4-1/2 in. long and 1 in. wide in over-all dimensions. The depression in the boat to hold the chromium was approximately 1-1/2 in. long and 1.4 in. wide with 1/8-in.-high sides. Up to 2 g of finely crushed chromium, an amount found to yield a coating approximately 40  $\mu$ in. thick with a source-to-substrate separation of 18 cm, could be evaporated from a boat of this design. Good electrical contact was made by clamping the boat leads lightly to heavy copper electrodes, which were capable of carrying a current of 100 amp. A boat charged with chromium and clamped between the electrodes is shown beneath the jig holding the cores to be coated in Figure 2. The boats were outgassed prior to loading with the chromium charge. Outgassing was carried out at a pressure of about 50  $\mu$ , while raising the boats to the temperature at which the chromium would be evaporated.

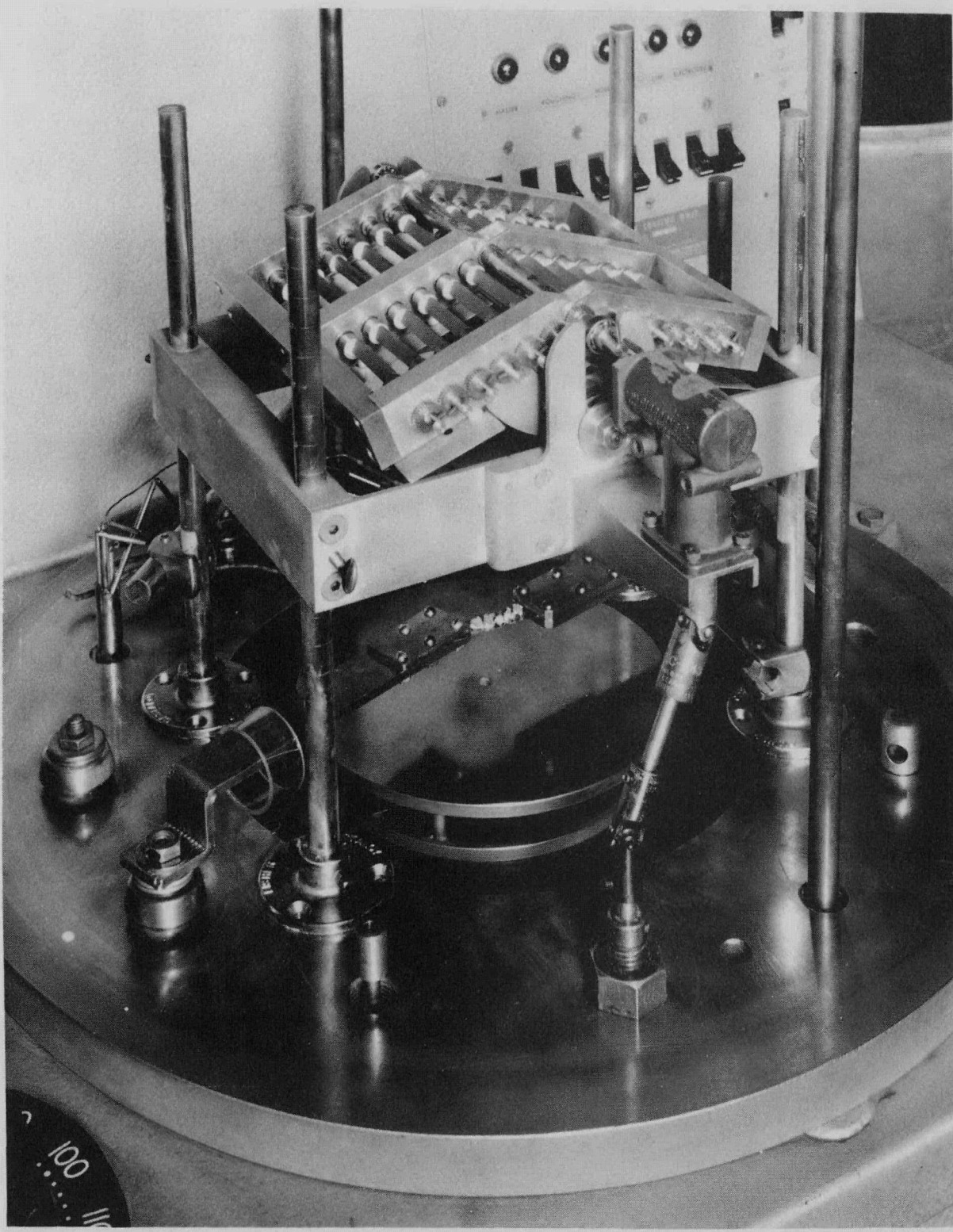
Because of the comparatively large amounts of chromium to be evaporated, the evaporation time often exceeded 1/2 hr. During this time, much heat was radiated by the filament heater with the consequent heating of the glass bell jar and other components in the system. To prevent the bell jar from overheating, a 5-in.-high shield made from 0.010-in.-thick molybdenum sheet was erected around the source to intercept the radiated heat.

As discussed above, it was necessary for economy to develop equipment which would rotate the cores in suitable position in the bell-jar chamber during the evaporation



N58794

FIGURE 1. APPARATUS USED FOR COATING URANIUM DIOXIDE CORES WITH CHROMIUM BY VACUUM EVAPORATION  
The bell-jar chamber is in the raised position.



1/2X

N58795

FIGURE 2. JIG USED TO INDIVIDUALLY MOUNT AND ROTATE THE  $UO_2$  CORES DURING VACUUM EVAPORATION OF CHROMIUM COATINGS ONTO THE CORES

The jig permitted 24 cores to be coated on four sides during a single evaporation. The chromium charge to be evaporated is shown beneath the cores in a molybdenum boat clamped between the electrodes.

in order that more than one side of the cores could be coated during one operation. The jig shown in Figure 2 was constructed in which 24 cores could be individually mounted and rotated so as to permit four sides of each core to be coated in a single evaporation. The jig was driven by a variable-speed electric motor located outside the vacuum chamber. The  $\text{UO}_2$  cores were individually held in the jig by frictional force. Rotational motion was imparted to the cores through interlocking gears linked to a central drive shaft. Greaseless bearings were used throughout. The ends of the cores were coated in separate evaporations by wrapping a large number of cores in aluminum foil and suspending them in one or more clamps above the source so that only the ends were exposed.

#### Coating Procedure

The chromium charge was placed in the previously outgassed molybdenum or tungsten boat, and the  $\text{UO}_2$  cores were suitably positioned, as shown in Figure 2. The bell-jar chamber was then secured in position and the system was evacuated. The temperature of the boat was raised by resistance heating until the chromium was vaporizing at an appreciable rate. After the chromium films had been deposited, the system was allowed to cool for 20 to 30 min before removing the cores. The coatings were then evaluated.

The amount of chromium evaporated was used to control the thickness. A chromium charge weighing between 1.5 and 2 g yielded a coating between 25 and 40  $\mu\text{in}$ . thick on the four exposed sides of the cores rotated in the jig with an average source-to-substrate separation of 18 cm. Since a film deposited on a stationary surface is approximately three times thicker than the film deposited on a uniformly rotating surface located at the same distance from the source, a much smaller chromium charge could be used for coating the ends of the cores. A chromium charge weighing between 0.3 and 0.5 g, at a source-to-substrate separation of about 15 cm, was used to yield the same thickness of coating on the ends of the cores.

Evaporations were begun when the pressure in the bell-jar chamber was less than  $5 \times 10^{-5}$  mm of mercury, and the pressure was not allowed to rise above  $1 \times 10^{-4}$  mm of mercury at any time during the film deposition. At higher pressures, the coatings were of poor quality. If during the evaporation, the pressure rose above  $1 \times 10^{-4}$  mm of mercury because of outgassing of heated components, the heater was turned off and the system was allowed to cool. When the system pumped down below  $5 \times 10^{-5}$  mm of mercury, the evaporation was begun again.

At a boat temperature of 1300 C, slight evaporation of the chromium could be detected. Between 1500 and 1700 C, the rate of evaporation was very rapid. Temperatures were measured with an optical pyrometer. The rate of evaporation was roughly indicated by the rate at which a chromium film was observed to be depositing on a glass microscope slide mounted in the system and also by direct observation of the chromium in the boat. A moderate rate of evaporation was found to be more desirable than a high rate, because it lessened the reaction between the molybdenum and chromium and thereby extended the boat life.

### Determination of the Thickness of the Coatings

The thickness of the coatings applied was determined from the weight increase of the core. It was assumed that the surfaces coated were smooth and that the density of the chromium film was approximately the same as the density of bulk chromium. Samples of the data used for the weight-gain calculations and the range of thicknesses obtained in two runs are shown in Table 1.

As expected for thin films, the electrical resistance of the coatings was found to vary inversely with the thickness. The results of resistance measurements were sufficiently consistent that an empirical curve could be plotted which approximated a theoretical curve calculated on the basis of the inverse variation of resistance with thickness. These curves are shown in Figure 3. The resistance of a coating was measured between the two clip leads, 1 in. apart, of an ohmmeter. No electrode termination was used. In the thickness range from 25 to 40  $\mu$ in., the resistance measured in this manner varied from about 5 to 33 ohms.

### Tests for Adherency of the Coatings

The principal method for judging the quality of adherence was visual examination. Peeling, flaking, or powdering were signs of nonadherence. If these signs of non-adherency were not evident, the coating was submitted to a cellulose-tape test and a smear test. The cellulose test consisted of placing the sticky side of ordinary cellulose tape against the coating and then removing the tape. If an appreciable amount of chromium was removed, the coating was considered to be nonadherent. If the removal was only very slight, the adherence of the coating was considered satisfactory, since the test is a severe one for this application. The smear test consisted of rubbing the coated core on a clean, white surface. If a dark smudge was produced, the coating was considered nonadherent. Little or no smudge was considered to indicate adherence.

### Results of the Preliminary Evaluation of the Coatings

The results of the preliminary evaluation of the coatings showed that by using developed procedures adherent coatings up to at least 100  $\mu$ in. thick could be applied to the surfaces of  $\text{UO}_2$  cores which had been sandblasted prior to coating. Thicker coatings were not investigated, since results from initial pressure-bonding tests of fuel elements containing cores with coatings 25 to 40  $\mu$ in. thick indicated that these coatings were adequate barriers to core-to-cladding reaction. Adherent chromium coatings with thicknesses in several ranges between 5 and 100  $\mu$ in. were applied to sandblasted  $\text{UO}_2$  cores to be evaluated in pressure-bonded elements to determine the minimum satisfactory thickness. Based on the results of the initial specimens, most of the coatings to be evaluated in bonded elements were approximately 25 to 40  $\mu$ in. thick and were applied to sandblasted cores. A few cores, however, were coated in this thickness range of 25 to 40  $\mu$ in. without being first sandblasted, and tests revealed the coatings to have satisfactory adherence, as good as those applied on the sandblasted cores. The results of the preliminary evaluation of the thickness and adherency of the vacuum-evaporated chromium coatings applied to  $\text{UO}_2$  cores to be evaluated in pressure-bonded fuel elements are presented in Table 2.

TABLE 1. SAMPLES OF DATA FOR CALCULATING<sup>(a)</sup> THE THICKNESS OF VACUUM-EVAPORATED CHROMIUM COATINGS

	Position A1(b)	Position A7	Position B6	Position B12
<u>Run Cr31</u>				
Weight of Core Plus Coating, g	6.22690	6.28415	6.32840	6.23320
Weight of Core, g	6.22355	6.27995	6.32425	6.22950
Weight of Coating, g	0.0035	0.00420	0.00215	0.00370
Thickness, cm	$6.9 \times 10^{-5}$	$8.6 \times 10^{-5}$	$8.5 \times 10^{-5}$	$7.6 \times 10^{-5}$
Thickness, A	6900	8600	8500	7600
Thickness, $\mu$ in.	27.2	34.0	33.7	30.0
<u>Run Cr32</u>				
Weight of Core Plus Coating, g	6.19555	6.27230	6.21420	6.22935
Weight of Core, g	6.19125	6.26730	6.20895	6.22435
Weight of Coating, g	0.00430	0.00500	0.00525	0.00500
Thickness, cm	$10.0 \times 10^{-5}$	$11.6 \times 10^{-5}$	$12.2 \times 10^{-5}$	$11.6 \times 10^{-5}$
Thickness, A	10,000	11,600	12,200	11,600
Thickness, $\mu$ in.	34.9	40.5	42.5	40.5

(a) The equation used for calculating the thickness, in centimeters, is

$$t = \frac{W}{Ad} ,$$

where W = weight of coating,

A = area of surface,  $\text{cm}^2 = 6.77 \text{ cm}^2$

d = density of chromium, g per  $\text{cm}^3 = 7.19 \text{ g per cm}^3$ .

(b) Positions are the locations of the cores in the jig. Positions A1 and B12 were at the ends; positions A7 and B6 were at the center.

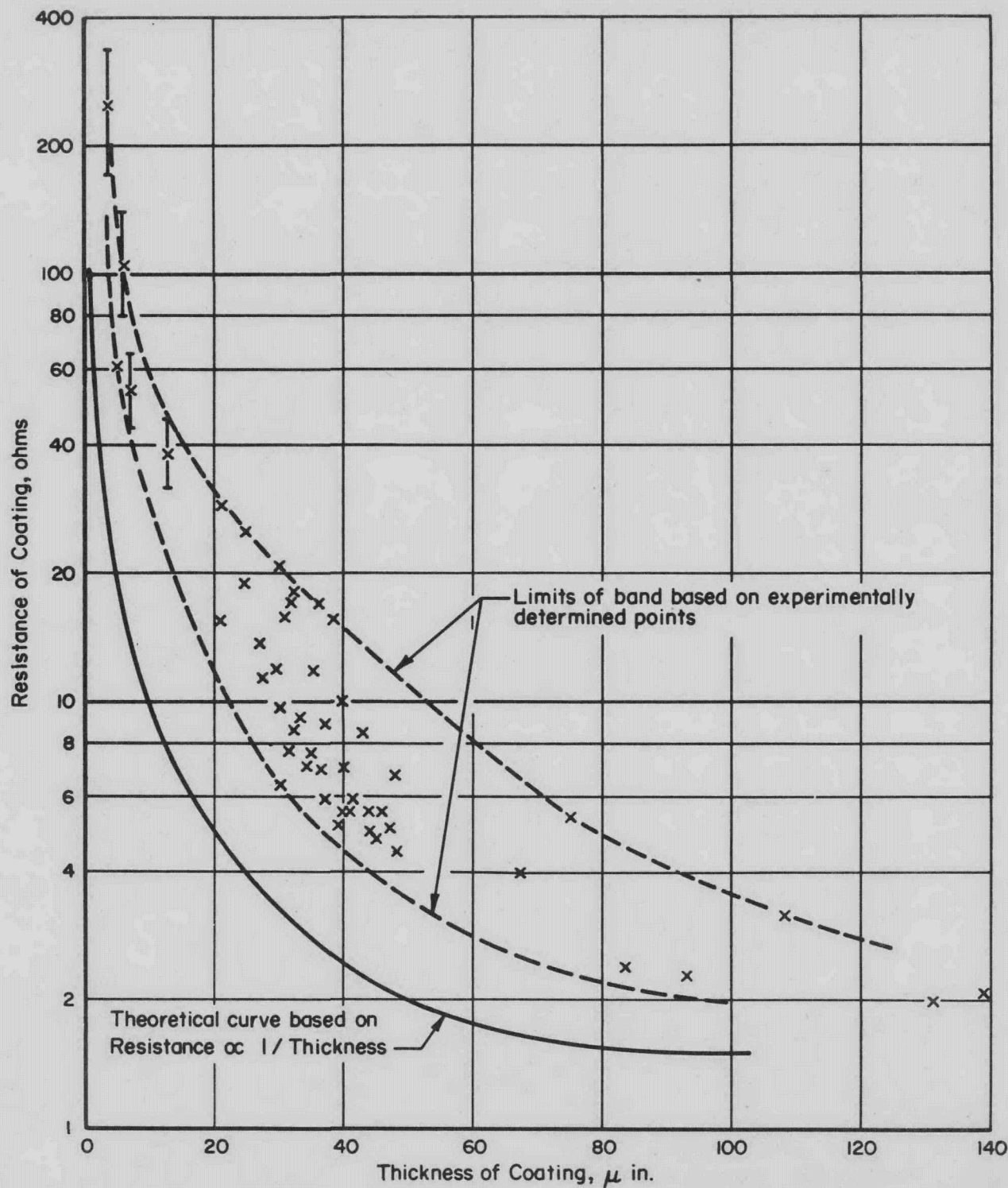


FIGURE 3. RESISTANCE VERSUS THICKNESS OF VACUUM-EVAPORATED CHROMIUM COATINGS ON  $\text{UO}_2$  CORES

The resistance indicated in this figure is the resistance measured with no electrode termination and with the clip leads of the ohmmeter spaced 1 in. apart.

TABLE 2. THICKNESS AND ADHERENCY OF THE VACUUM-EVAPORATED CHROMIUM COATINGS APPLIED TO URANIUM DIOXIDE CORES TO BE EVALUATED IN PRESSURE-BONDED FUEL ELEMENTS

Run	Number of Cores		Adherence	Thickness, μin.	Resistance Range, ohms
	Sandblasted	As Sintered			
Cr6	15	--	Good	5-10	44-65
Cr7	15	--	Good	10-15	32-46
Cr8	12	--	Good	65-95	2.2-4.1
Cr10	13	--	Good	45-50	2.1-14
Cr11	17	--	Good	25-30	9.2-13
Cr13	17	--	Good	20-25	23-29
Cr14	19	--	Good	30-35	15-21
Cr15	21	--	Good	30-33	18-33
Cr16	22	--	Good	25-30	11-17
Cr17	21	--	Good	25-28	12-20
Cr18	21	--	Good	35-40	16-25
Cr20	22	--	Good	40-50	4.4-7.1
Cr21	21	--	Good	35-40	5.2-9.2
Cr22	18	--	Good	33-38	6.8-8.6
Cr23	22	--	Good	35-45	7.4-12
Cr24	18	--	Good	25-30	13-19
Cr24	--	3	Good	25-30	18-19
Cr25	17	--	Good	30-35	7.4-12
Cr25	--	2	Good	30-35	7.8-11
Cr26	11	--	Good	35-37	8.7-12
Cr26	--	10	Fair	35-37	9.7-16
Cr27	11	--	Good	35-40	7.3-11
Cr27	--	9	Good	35-40	8.0-10
Cr28	8	--	Good	30-35	5.9-7.8
Cr28	--	11	Good	30-35	5.7-8.1
Cr29	12	--	Good	35-40	15-18
Cr29	--	7	Good	35-40	17-19
Cr30	13	--	Good	30-45	4.9-9.0
Cr30	--	7	Fair	30-45	5.7-7.5
Cr31	13	--	Good	25-35	7.1-12
Cr31	--	7	Good	25-35	7.2-11
Cr32	13	--	Good	35-45	4.9-7.0
Cr32	--	7	Good	35-45	3.9-6.3
Cr33	13	--	Good	30-35	6.9-8.6
Cr33	--	7	Good	30-35	7.3-8.9
Cr34	--	20	Good	25-45	14-29
Total	405	90			

Development of the Pyrolytic Process for Coating Uranium Dioxide  
Cores with Crystalline Carbon

Thin coatings of crystalline carbon can be applied to uranium dioxide cores by the thermal decomposition or cracking of methane gas at 1025 C in a fused-quartz reaction tube placed inside an electrically heated temperature-controlled furnace. Pure carbon in a crystalline form is deposited on the surfaces of the cores, while hydrogen and intermediate products formed in the dehydrogenation of methane are vented as furnace gases. This process was selected for investigation because the carbon coating applied was expected to be an adherent and effective barrier to reaction based on known properties and because the process is an inexpensive industrial method for producing carbon-film resistors. The coatings applied under various conditions were subjected to preliminary evaluations to determine their thickness and adherence. The results are reported later in this discussion. Those coatings which appeared satisfactory were then applied to a large number of cores and evaluated on the basis of their behavior in gas-pressure-bonded fuel elements, as reported in a later section of this report.

Materials and Equipment

In the coating operation, a cylindrical furnace which was electrically heated by Carborundum elements was employed. A Foxboro temperature controller, connected to a thermocouple located in the hot zone of the furnace, maintained the temperature of 1025 C. A fluctuation of  $\pm 5$  C was recorded. The cracking of the methane gas and deposition of the carbon coatings occurred inside a fused-quartz tube in which the longitudinal axis coincided with that of the furnace. The outside diameter of the quartz tube was 1-3/4 in.; the inside diameter was about 1-1/2 in. Rubber stoppers, with glass-tubing feedthroughs, were used to seal the reaction tube from the atmosphere. The  $\text{UO}_2$  cores to be coated were arranged in a wire rack placed in a fused-quartz boat. The boat could be moved into and out of the coating zone of the reaction tube by means of a long tungsten rod without opening the system to air. Glass wool packed around the push rod furnished the seal. Six cores were coated at one time with the apparatus used in this study.

The gases used in the process were commercial-grade methane which had a purity of 93 per cent or greater and commercial-grade dry nitrogen. Nitrogen served as a flushing gas for removing air from the system and as a mixing or carrier gas during the coating process to assist the flow of methane through the reaction tube. The  $\text{CH}_4$  and the nitrogen for mixing, both of which entered at one end of the quartz tube, had flow rates of 50  $\text{cm}^3$  per min and 200  $\text{cm}^3$  per min, respectively. The nitrogen for flushing entered from the opposite end and had a flow rate of 170  $\text{cm}^3$  per min.

Sandblasting of the Cores Prior to Coating

As a part of the coating procedures, the surfaces of most of the  $\text{UO}_2$  cores were uniformly roughened by a sandblasting operation, which was thought to improve the adherency of the coatings. However, some cores were coated with the surfaces in the as-pressed-and-sintered condition. The sandblasting operation was performed with an

S. S. White Industrial Airbrasive unit, Model C, using their Powder No. 1. The cores were blasted inside an enclosure which was continuously exhausted during the operation. A glass sight window on the top of the enclosure provided an unobstructed view. The nozzle was held approximately 1/2 in. from the surfaces of the as-sintered cores and passed lightly two or three times over each point on the surfaces. This was sufficient to remove the shiny areas observed and to uniformly roughen the surface. After being sandblasted, the cores were blown with air and brushed to remove dust.

#### Coating Procedure

Studies of the deposition of carbon films have shown that certain conditions of temperature and methane concentration will produce a preferential crystal orientation, for which the pyrolytic carbon film will have a maximum hardness. These conditions were selected for the deposition of pyrolytic carbon coatings on the  $\text{UO}_2$  cores.

The coating procedure was as follows: First, the furnace was heated to 1025 C and the flow of nitrogen from both ends of the tube was started. The flow of nitrogen was maintained from both ends during all stages of the coating process. The boat was loaded with the cores to be coated, and the reaction tube was then sealed from the atmosphere. After 5 min in the cool zone, during which time the air was flushed out of the system, the cores were advanced into the hot zone in the center of the tube for 15 min of preheating. The methane flow was then turned on for a suitable length of time during which the cracking of the methane and the deposition of the carbon coatings took place. The length of the deposition time was varied to control the thickness of the coating. At the end of the deposition, the boat was moved to the cool zone and the methane was turned off. After a 5-min cooling period, the system was opened, and the coated cores were removed. It was not necessary to cool the furnace, and, since the deposition was carried out at atmospheric pressure, the boat could be reloaded and a new run started immediately.

Care was taken to keep the system free of oxygen during the deposition; otherwise, soot formation occurred and resulted in powdery, nonadherent coatings. The best coating zone was found to be in the lower half of the tube. Sooty coatings were formed on the portions of the cores extending very far into the upper half. Sometimes sooty coatings appeared on the cores in the first run after starting the equipment in operation, while succeeding runs would yield good-quality coatings. To assure that the coating apparatus was functioning properly, the first run was made as a conditioning run with only a Vycor substrate in the boat.

#### Techniques for Measuring the Thickness of the Coatings

The thicknesses of the pyrolytic crystalline-carbon coatings were determined by two indirect methods. One method depended upon the relationship between the thickness of a carbon film and its resistance. To measure the resistance of a film, silver electrodes were painted on the ends of a coated core with a 1-in. length of film left unpainted. The electrodes were then held in the clip leads of an ohmmeter. The resistance of the film was also measured without any terminal electrodes by holding the core with the clip leads 1 in. apart and was found to be approximately 1-1/3 times the resistance measured with terminal electrodes. The film resistance per unit area was then calculated using the appropriate dimensions and the resistance measured with electrode terminals, or the resistance measured without electrode terminals times the

experimental conversion factor of 3/4. The corresponding film thickness could then be determined using published data for thickness versus film resistance per unit area for pyrolytic carbon films.(7)

The second method used to measure the coating thickness was the standard method developed by Tolansky(8) for measuring the thickness of thin films. This method involved multiple-beam interferometry measurements made of Vycor substrates which had been coated simultaneously with some of the uranium dioxide cores.

#### Tests for Adherency of the Coatings

The primary test for adherency of the pyrolytic carbon was a visual examination of the coatings. An adherent coating appeared uniformly grey and even. If the coating appeared bubbled or blistered, it peeled readily. The cellulose-tape and smear tests were conducted as described in the section on chromium coatings. As was the case for the tests of the chromium coatings, these adherency tests provided only an estimate of the quality of adherency.

#### Results of the Preliminary Evaluation of the Coatings

An exploratory study of the pyrolytic coating process was directed toward obtaining nonporous and adherent crystalline-carbon coatings of different thicknesses by varying the deposition time. Other variables, such as methane concentration and temperature, were held constant. The results of this study are summarized in Table 3. It was found that only very thin coatings approximately 1  $\mu$ in. thick, corresponding to a deposition time of 2 min, were consistently adherent when deposited on cores with as-sintered surfaces. Thicker coatings did not adhere to shiny, glazed portions of the surfaces of the cores. In order to deposit thicker coatings which were adherent, it was necessary to first roughen the surfaces of the cores by sandblasting. Adherent coatings of crystalline carbon were applied to sandblasted cores to a maximum thickness of about 15 to 40  $\mu$ in., corresponding to a deposition time of 20 min. Coatings much thicker than these were not adherent, even on roughened cores.

Since the initial pressure-bonded elements containing sandblasted cores coated with carbon using a 20-min deposition time appeared satisfactory, a large number of cores were coated for this time interval and assembled into fuel elements to be pressure bonded and evaluated. Also, a sufficient number of cores with as-sintered surfaces were coated with about 1  $\mu$ in. of carbon using a deposition time of 2 min to be evaluated in a pressure-bonded element.

The results of the preliminary evaluation of the thickness and adherency of the coatings on these cores which were prepared for assembly into fuel elements are included in Table 3. The results of the thickness measurements made of these coatings using the multiple-beam interferometry and the film-resistance techniques are also contained in the table. It was found that the results of the multiple-beam interferometry measurements of the films deposited in 20 min indicated them to be thinner than did the resistance measurements. The lack of complete agreement is not unexpected, since both techniques are indirect methods of determining the coating thickness on the uranium dioxide cores. The difference in the results, therefore, could be due to a difference in

TABLE 3. SUMMARY OF RESULTS OF THE PRELIMINARY EVALUATION OF THE THICKNESS AND ADHERENCE OF PYROLYTIC CARBON COATINGS ON URANIUM DIOXIDE CORES

Deposition Time, min	Surface Condition of Cores	Number of Cores Coated	Adherence of Coating	Resistance Range (Measured Without Terminals), ohms		Coating-Thickness Range, $\mu$ in.	
				Based on Film Resistance	Based on MBI <sup>(a)</sup>	Based on Film Resistance	Based on MBI <sup>(a)</sup>
1	Sandblasted	3	Good	2400-4000			
	As sintered	3	Good	2800-3800			
2	Sandblasted	3	Good	1200-1500			
	As sintered <sup>(b)</sup>	73	Good	700-1900	0.5-1.4		1-1.5
5	Sandblasted	3	Good	220-260			
	As sintered	3	Fair	220-260			
10	Sandblasted	9	Good	68-90			
	As sintered	3	Poor	80-100			
15	Sandblasted	3	Good	50-56			
	As sintered	3	Poor	62-80			
20	Sandblasted <sup>(b)</sup>	605	Good	25-70		15-40	
	As sintered	8	Poor	38-50			15
30	Sandblasted	3	Poor	18-24			
	As sintered	--					
45	Sandblasted	8	Poor	11-40			
	As sintered	--					
60	Sandblasted	7	Poor	12-20			
	As sintered	3	Poor	16-17			
180	Sandblasted	1	Poor	7.5			
	As sintered	--					

(a) Multiple-beam interferometry measurements.

(b) The cores having coatings applied under these conditions were evaluated in gas-pressure-bonded fuel elements.

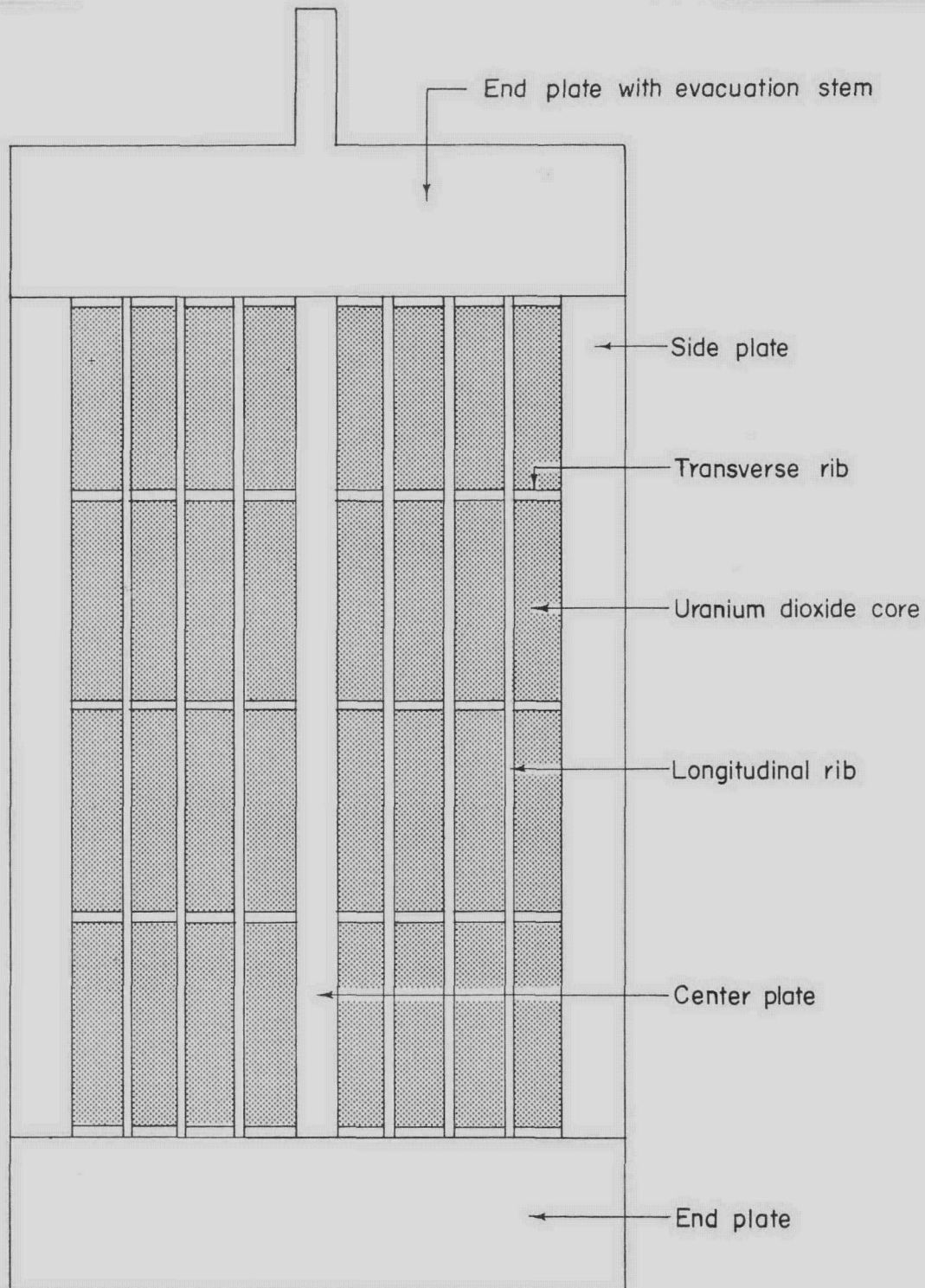
deposition rate on the Vycor substrates used for the multiple-beam interferometry measurements as compared to the uranium dioxide cores, or due to inherent inaccuracy in the resistance measurements of the films or their conversion to film thicknesses. The resistance measurements of the films were found to be reproducible, however, and this relatively simple technique could probably be used for control purposes in a production operation to insure that coatings of the desired thickness and quality are being obtained.

#### BOND-TEST RESULTS WITH PYROLYTIC CARBON, VAPOR-DEPOSITED CHROMIUM, AND GRAPHITE COATINGS

In order to evaluate the various types of core coatings and to determine the reproducibility of the Zircaloy-to-Zircaloy bonds in fuel elements prepared with the different coatings, 36 fuel elements were prepared and bonded. The components used for these elements and their preparation are described in more detail in the section on cleaning and assembly; however, the type of element is illustrated in Figures 4, 5, and 6. Figure 4 shows a drawing of the piece-component picture-frame configuration, and Figures 5 and 6 are photographs of the components before and after assembly, respectively.

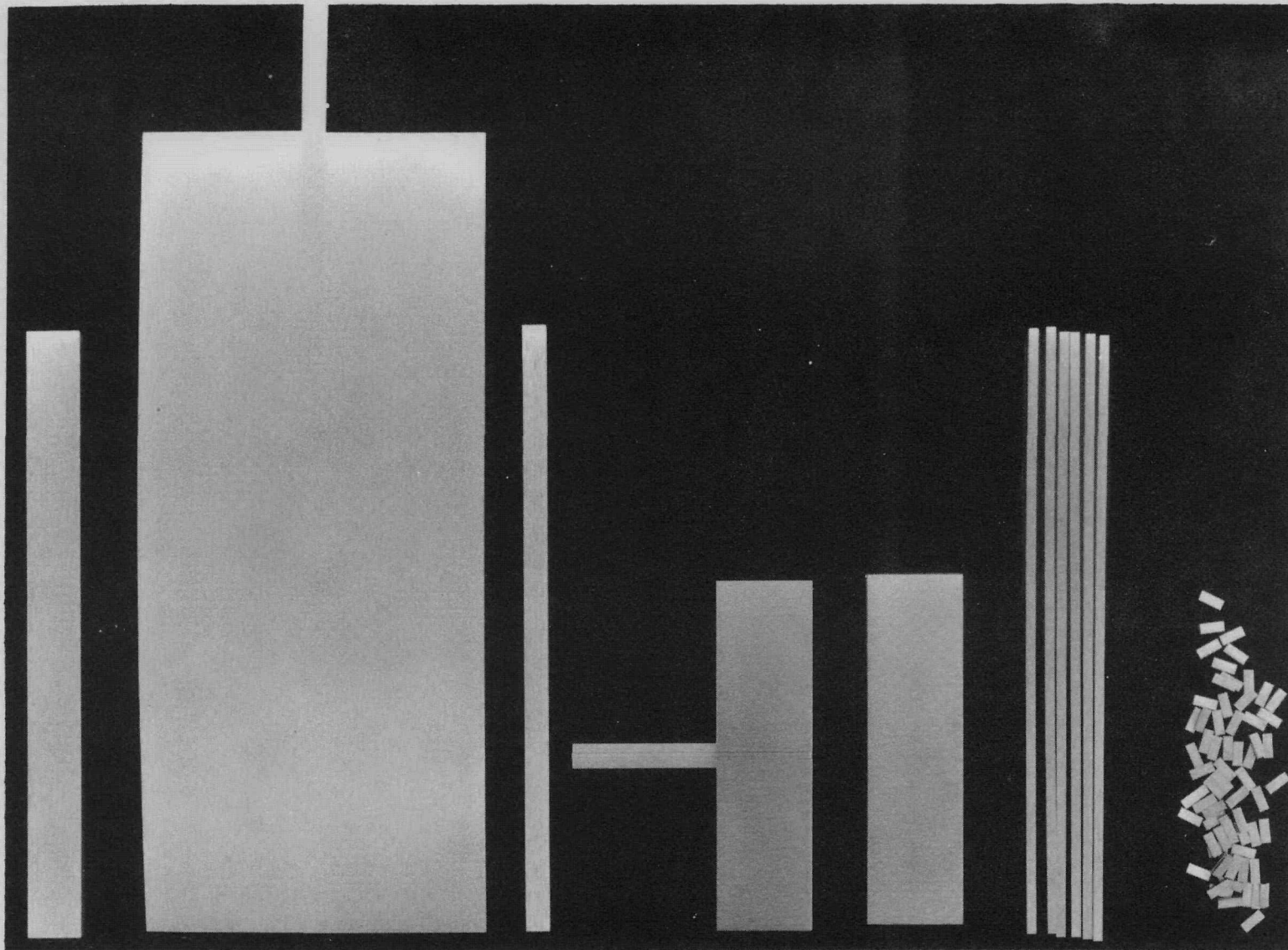
Each fuel element was assembled containing cores which all had the same type of barrier coating, and an approximately equivalent number of elements were prepared containing cores with each of three types of coatings. The coatings employed were sprayed, buffed graphite, pyrolytic crystalline carbon, and vacuum-evaporated chromium. All were applied by the techniques previously described. It was desired to determine the effectiveness of each of the coatings in preventing core-to-cladding reaction and their effect, if any, on the quality of the Zircaloy-to-Zircaloy bonds in the elements. The sprayed and buffed graphite-coated cores were used as a basis of comparison for the coating effectiveness. This coating was studied previously as reported in BMI-1374.(2) It was the intent of this development study to determine if better and more effective coatings could be developed.

Of the 36 fuel elements prepared in this study, 15 contained chromium-coated cores, 14 contained crystalline-carbon-coated cores, and 7 contained graphite-coated cores. The chromium coatings evaluated were applied in several thickness ranges and were applied to cores which had and had not been sandblasted prior to coating. The sprayed and buffed graphite coatings were applied only to cores which had not been sandblasted and were of only one thickness, 5 mg per in.<sup>2</sup>. Pyrolytic crystalline-carbon coatings were bonded which were about 15 to 40  $\mu$ in. thick on sandblasted cores and about 1  $\mu$ in. thick on cores which had as-sintered surfaces. The earlier elements in the series were evaluated in both the as-bonded condition and after an additional 5-min heat treatment at 1850 F. Earlier studies(2) had indicated the added heat treatment might improve the integrity of the clad fuel element. It was desirable and the intent of this study, however, to eliminate this added treatment, since it would be an expensive operation in production and would involve problems of dimensional distortion and contamination of the cladding. The fuel elements prepared were intensively evaluated by metallographic examinations, burst tests, corrosion and intercompartmental-leakage tests, and chemical analyses.



0-25928

FIGURE 4. DRAWING OF THE CONFIGURATION OF THE PIECE-COMPONENT PICTURE FRAME CONTAINING URANIUM DIOXIDE CORES



2/3X

Two side  
plates

Two cladding  
plates

One center  
plate

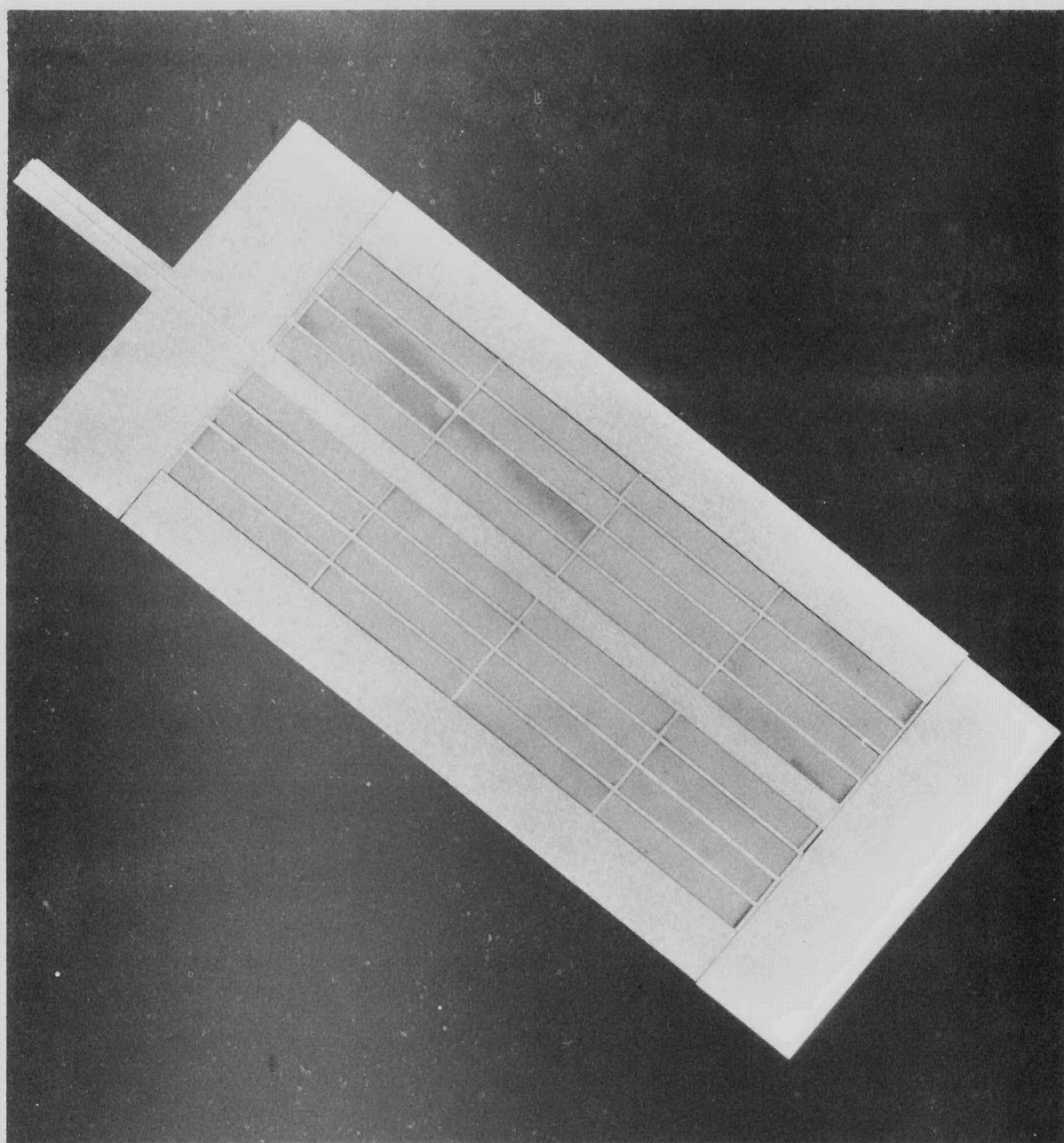
One end plate  
with evacuation  
stem and groove

One end  
plate  
(bottom)

Six longi-  
tudinal  
ribs

N64738  
Forty  
transverse  
ribs

FIGURE 5. THE ZIRCALOY-2 CLADDING COMPONENTS FOR A FUEL ELEMENT OF THE TYPE PREPARED IN THIS STUDY



2/3X

N64736

FIGURE 6. PICTURE FRAME ASSEMBLED FROM PIECE ZIRCALOY CLADDING  
COMPONENTS CONTAINING THE URANIUM DIOXIDE CORES

Void spaces in the picture frame were eliminated by shimming and  
by shifting the components during the final steps of assembly.

Metallographic Examination

Cross-sectional samples were taken from several locations of the fuel elements containing the three types of coated cores for metallographic examination of the quality of the Zircaloy-to-Zircaloy bonds and the extent of core-to-cladding reaction. The quality of the bonds in the elements was classified by the percentage of areas with bonds designated as Types A, B, and C. The original interface of a Type A bond is not visible metallographically; there is complete grain growth across the entire original bond interface and no visible contamination or voids at the interface. An area of a bond classified as Type B has grain growth across the bond interface, but slight contamination or voids are visible along the original bond line. An area of a bond which does not demonstrate grain growth across the interface, with or without visible bond-line contamination or voids, is designated as Type C. Typical bonds of each type are shown in Figure 7.

As-bonded, as well as heat treated, elements containing cores with the three types of coatings exhibited excellent Zircaloy-to-Zircaloy bonds, showing grain growth across almost the entire original interface in all locations with a minimum amount of bond-line contamination. Thus, the results showed that all three coatings generally permitted equivalent, high-quality Zircaloy-to-Zircaloy bonding. The results of these metallographic examinations of the Zircaloy-to-Zircaloy bonds in the as-bonded and as-heat-treated specimens revealed that all of the fuel elements contained a high percentage, normally about 90 to 95 per cent, of Type A bonds, according to the classification system described in Figure 7. Some areas of bond classified as Type B were observed, and small isolated areas of Type C bond were detected. Most of these areas, although infrequent, were observed in the bonds between the transverse ribs and the longitudinal ribs, indicating the importance of surface preparation and cleaning of all bonding surfaces of these components. None of the specimens contained a significant amount of Type C bond, as would be expected on the basis of the excellent strength revealed by all of the bonds which were burst tested.

Since the elements containing the three types of core coatings were observed to have equivalent bonding, it was indicated that none of the three had any adverse effect on the bonds in the elements. Also, as-bonded and as-heat-treated specimens both consistently contained bonds of comparable high quality, demonstrating that the additional 5-min heat treatment in an 1850 F salt bath, which would be an undesirable operation in production, was not necessary. Typical areas of the bonding observed in these specimens are illustrated in the photomicrographs of Figures 8 and 9 for specimens in the as-pressure-bonded condition and after a 5-min heat treatment in an 1850 F salt bath, respectively. The representative area of bonding in an as-pressure-bonded element is shown in Figure 8 using both bright-field and polarized illumination, since the former best reveals any contamination present in the bond interface, and the latter shows the extent of grain growth across the interface.

Also bonded in this series of elements was one specimen containing sandblasted cores coated with pyrolytic carbon which was prepared so as to determine if the Zircaloy bonding surfaces could be contaminated by the core coatings due to mishandling during assembly. During assembly of this element, the cores were rubbed against the relatively rough bonding surfaces of the bottom Zircaloy cladding plate. Also, after the cores and receptacle-plate components were in position, the entire top surface of the

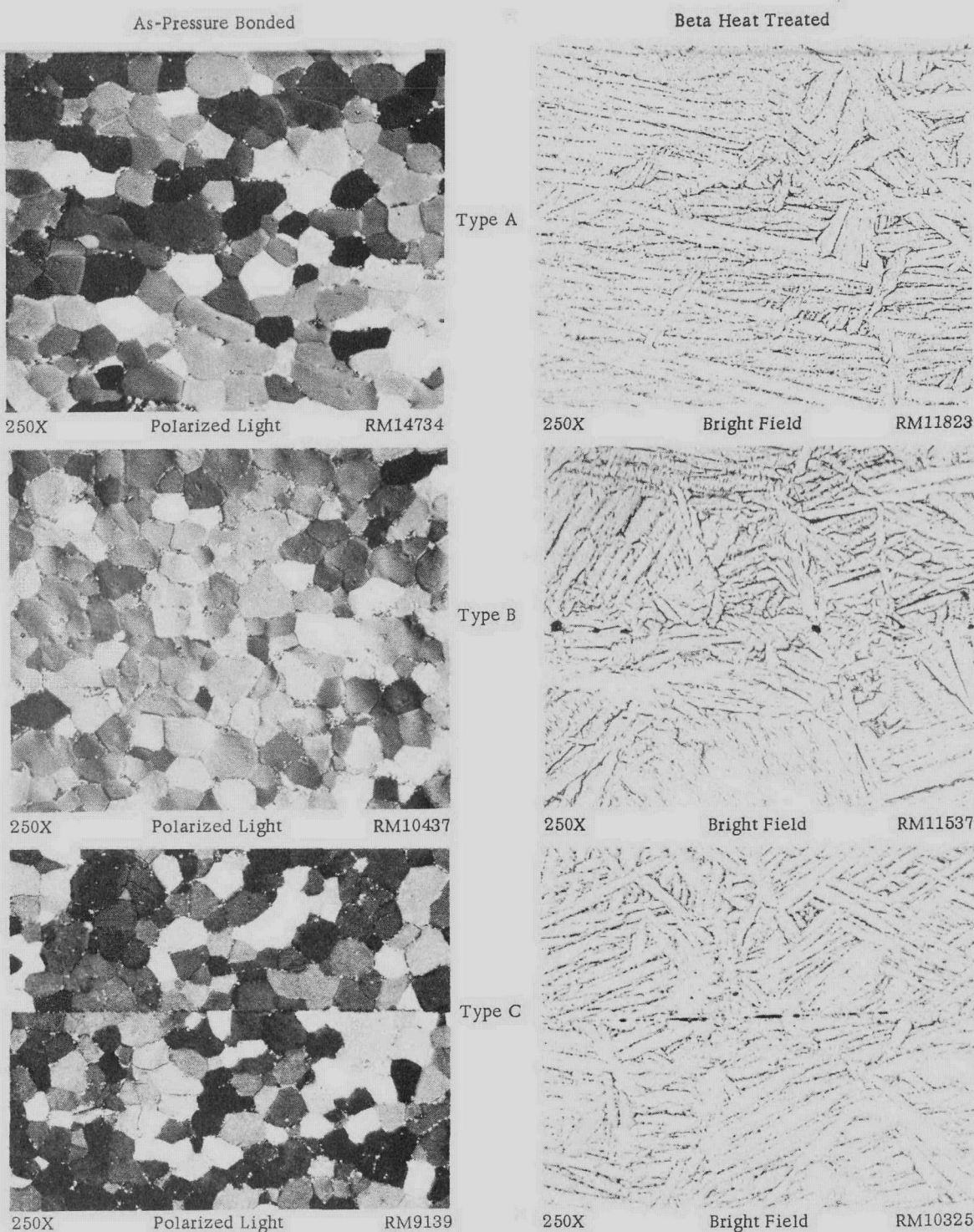


FIGURE 7. CLASSIFICATION OF BONDS AS TYPES A, B, AND C BY METALLOGRAPHIC EVALUATION

Type A - Grain growth across entire bond interface, no visible bond-line contamination or voids.

Type B - Grain growth across bond interface, bond-line contamination or voids visible.

Type C - No grain growth across bond interface, with or without visible bond-line contamination or voids.

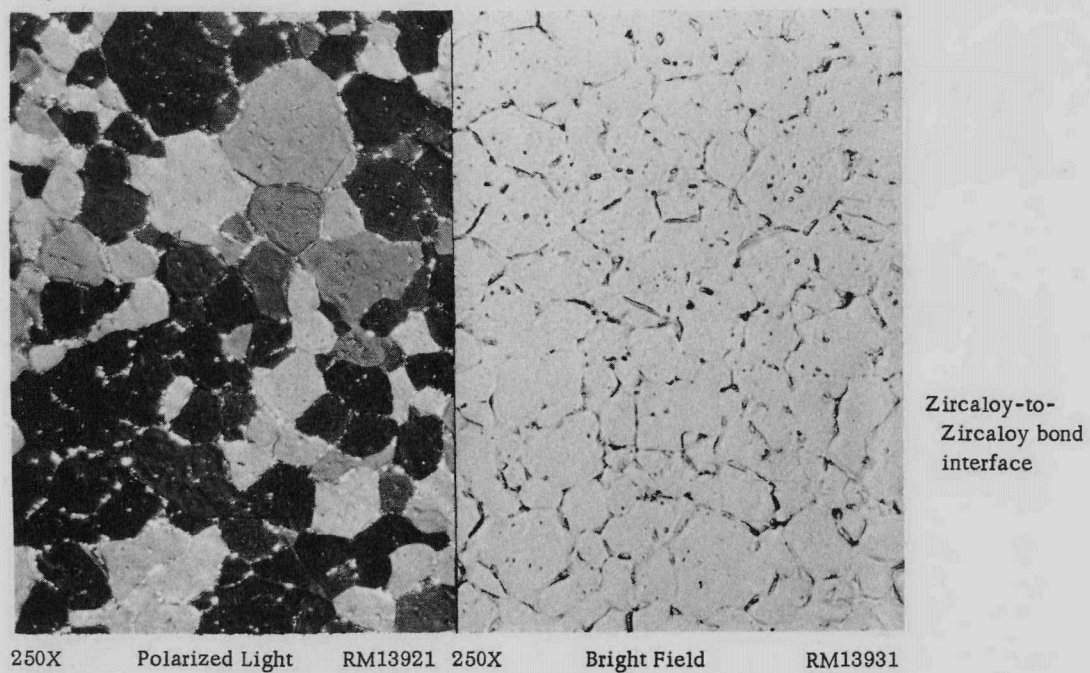


FIGURE 8. TYPICAL ZIRCALOY-TO-ZIRCALOY BOND OF THE EXCELLENT QUALITY OBTAINED IN GAS-PRESSURE-BONDED FUEL ELEMENTS PREPARED BY THE DEVELOPED TECHNIQUES

Right portion of figure (bright field illumination) shows that there was no bond-line contamination, and left portion (polarized-light illumination) shows that there was grain growth across the original bond interface.

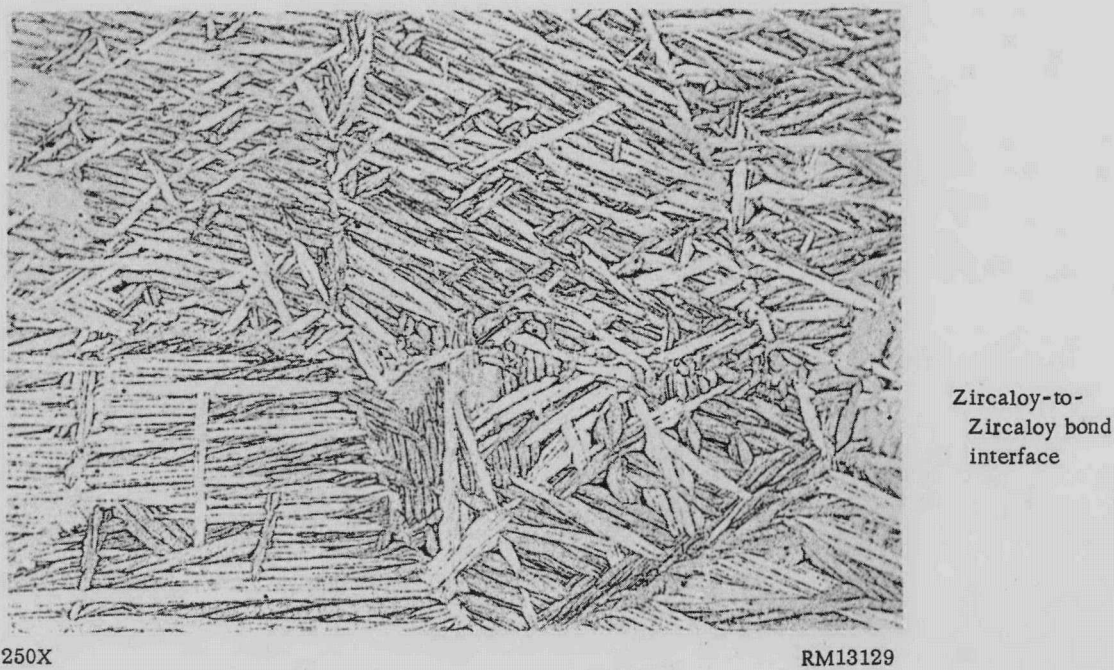


FIGURE 9. TYPICAL ZIRCALOY-TO-ZIRCALOY BOND OBSERVED IN FUEL ELEMENTS WHICH WERE GAS-PRESSURE BONDED AND SUBSEQUENTLY HEAT TREATED FOR 5 MIN IN AN 1850 F SALT BATH

No bond-line contamination was present, and grain growth occurred across the entire original bond interface.

cores and ribs was rubbed using rubber gloves in an attempt to transfer carbon from the cores onto the surfaces of the ribs. Metallographic examination revealed no contaminated bonds in this element, demonstrating that these coatings were very adherent and satisfactory for use in a production operation. Also, the burst tests of this element, as reported in a subsequent section of this report, did not result in any bond failures, indicating that the bonds were very strong. Chromium coatings because of their nature do not result in contamination of the bonds. Graphite coatings would not be as suitable for production, since previously reported results<sup>(2)</sup> for several elements which were purposely mishandled during assembly showed that this coating could be smeared by mistreatment onto the Zircaloy bonding surfaces and interfere with bonding. These elements with the smeared graphite coatings were observed metallographically to contain contaminated bonds exhibiting a lack of grain growth across the interface, and these bonds failed during burst testing, showing that they were weak. On this basis, core coatings of crystalline carbon or chromium would be preferable in a production process to the buffed-graphite coatings.

No core-to-cladding reaction was observed in as-bonded or as-heat-treated specimens with proper core coatings of crystalline carbon, evaporated chromium, or buffed graphite, except for very slight apparent reaction occasionally at the corner of a core. The frequency of reaction at the core corners was slightly greater for the buffed graphite coatings than for either of the other coatings; however, the reaction was normally slight and the occurrence not very frequent. As-bonded and as-heat-treated specimens with 25 to 100- $\mu$ in. -thick chromium coatings on the cores showed no core-to-cladding reaction, although the heat-treated specimens revealed diffusion of chromium into the Zircaloy. As-bonded and as-heat-treated specimens with 5 to 10- $\mu$ in. -thick coatings of chromium exhibited some core-to-cladding reaction in general areas. Crystalline-carbon coatings in the thickness range of 15 to 40  $\mu$ in. prevented reaction in as-bonded and as-heat-treated elements; crystalline-carbon coatings only 1  $\mu$ in. thick, which were applied to the cores contained in one element, permitted considerable reaction to occur during pressure bonding. All of the sprayed and buffed graphite coatings were applied in the amount of 5 mg of graphite per in.<sup>2</sup> of core surface (approximately 800  $\mu$ in. thick), which had previously been found<sup>(2)</sup> to be the optimum coating thickness to obtain the most adherent coating and still prevent reaction in as-bonded and as-heat-treated elements.

A typical as-pressure-bonded interface between a Zircaloy-2 cladding plate and uranium dioxide core coated with 15 to 40- $\mu$ in. -thick crystalline carbon is shown in Figure 10. Normally there was no visible evidence of reaction even at the corners of the crystalline-carbon-coated cores, as illustrated by the photomicrograph in Figure 11 of an as-bonded specimen and in Figure 12 of an as-heat-treated specimen. These regions at the corners of cores evidently are especially susceptible to reaction, however, and slight reaction apparently occurred in a few such areas. This is illustrated in Figure 13 which reveals adjacent to the corner of the core a zone of Zircaloy which has a changed structure, interpreted as an indication that the zone had a high oxygen content as a result of core-to-cladding reaction. The amount of reaction must have been slight, since there is no visible zone of uranium-zirconium reaction products. The excellent Zircaloy-to-Zircaloy bonds obtained in the specimens containing crystalline-carbon coated cores can also be observed in Figures 11, 12, and 13, which show portions of the bond interfaces between a Zircaloy cladding plate and a rib of the piece-component picture frame in three typical elements.

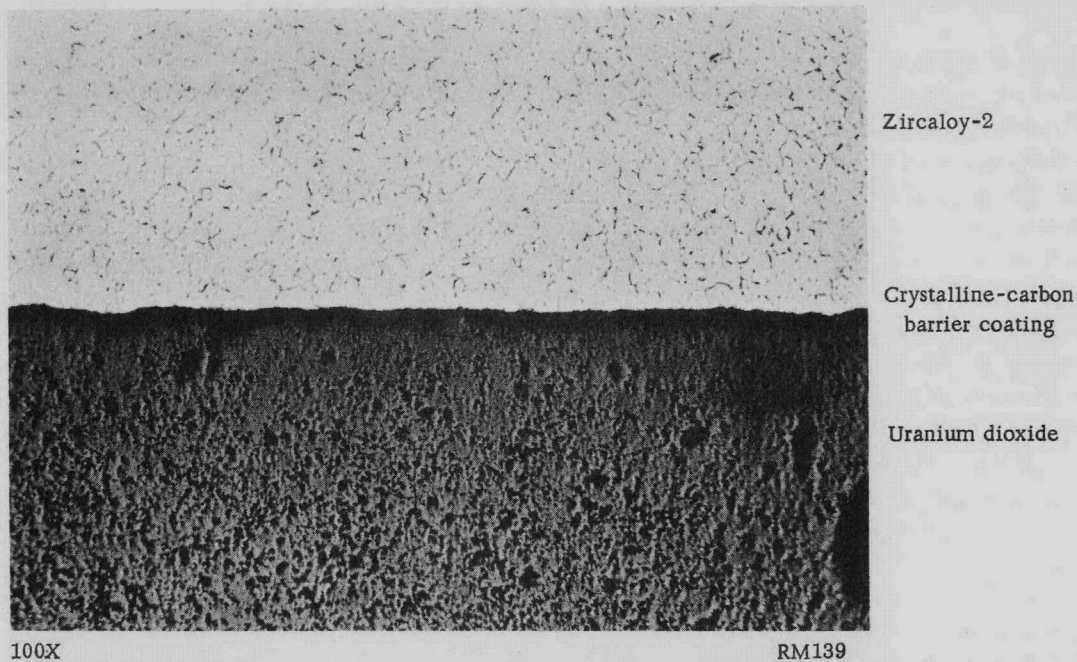


FIGURE 10. TYPICAL AS-PRESSURE-BONDED INTERFACE BETWEEN A ZIRCALOY CLADDING PLATE AND A URANIUM DIOXIDE CORE COATED WITH 15 TO 40- $\mu$ IN.-THICK CRYSTALLINE CARBON

No core-to-cladding reaction occurred.

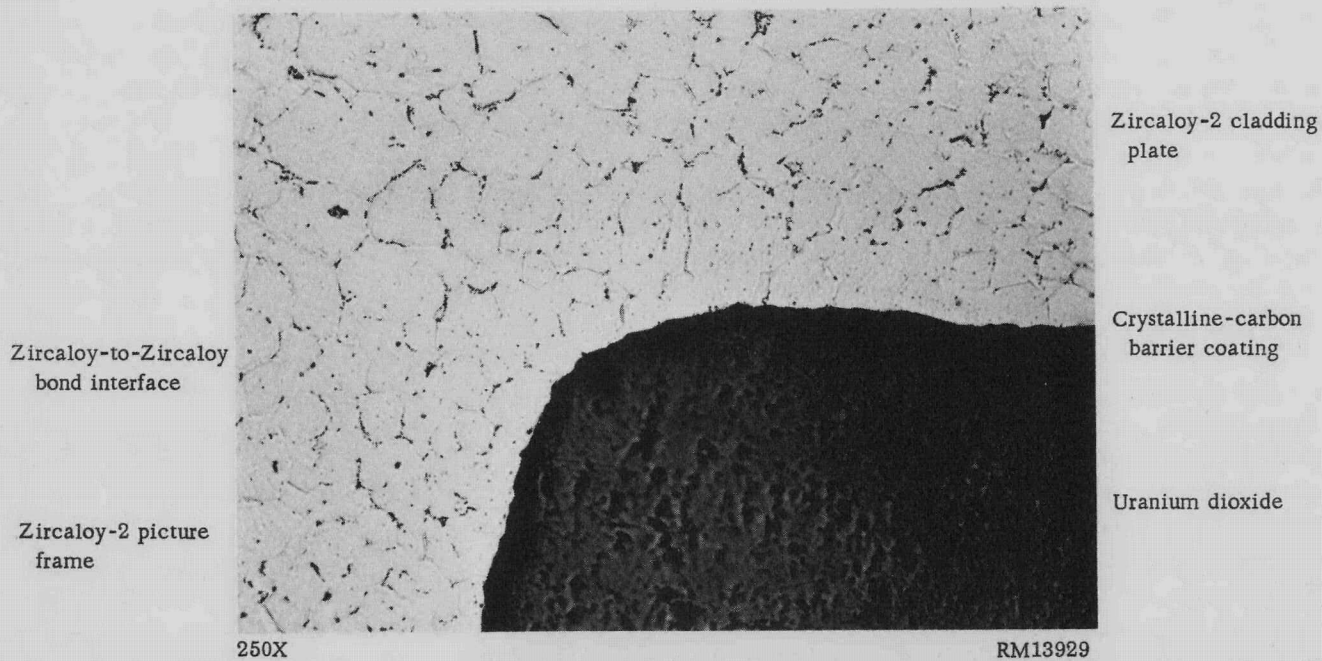
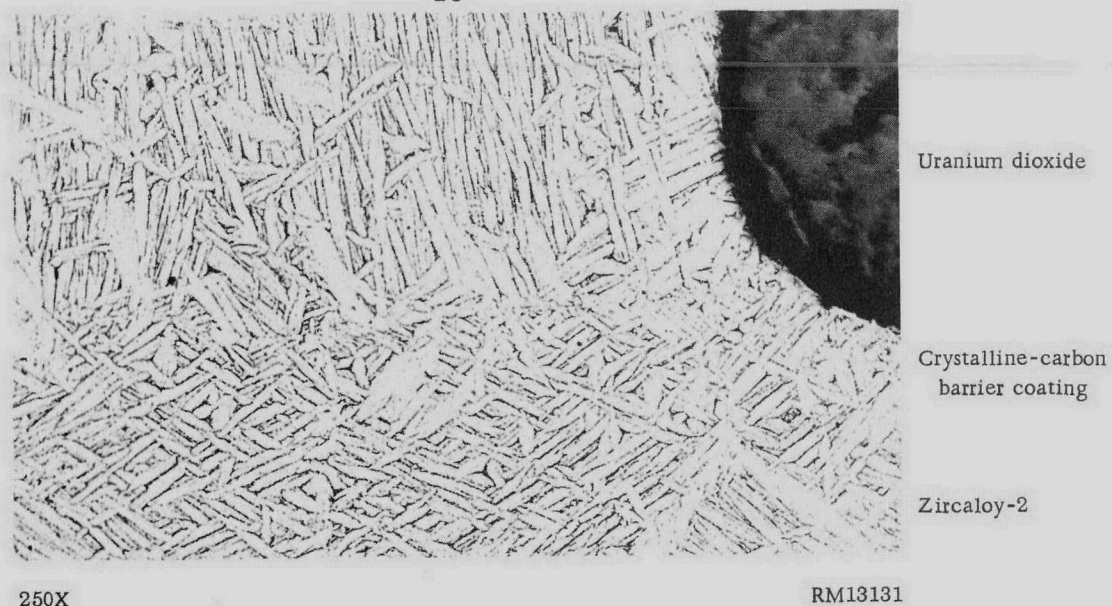


FIGURE 11. TYPICAL INTERFACE BETWEEN THE ZIRCALOY CLADDING COMPONENTS AND THE CORNER OF A CRYSTALLINE-CARBON-COATED URANIUM DIOXIDE CORE IN A GAS-PRESSURE-BONDED FUEL ELEMENT

Thickness of the crystalline-carbon coating on the core was 15 to 40  $\mu$ in. Note the lack of any core-to-cladding reaction and the good Zircaloy-to-Zircaloy bond.

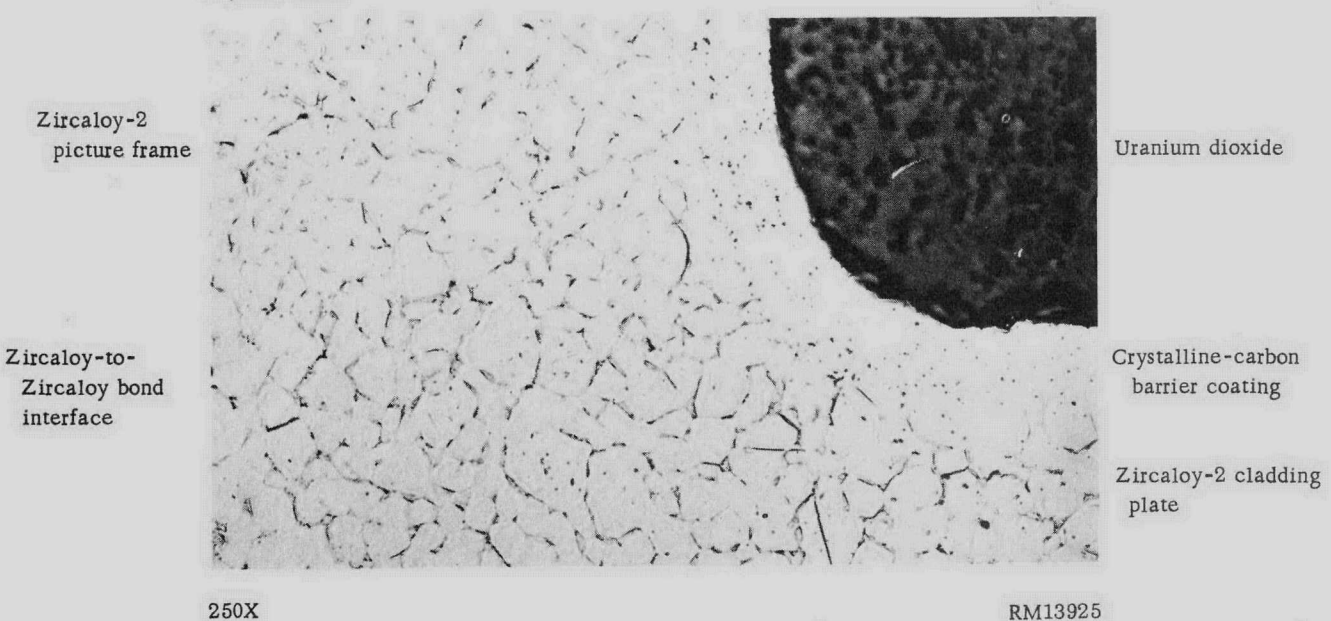


250X

RM13131

FIGURE 12. AREA SIMILAR TO THAT SHOWN IN FIGURE 11 IN A FUEL ELEMENT WHICH WAS HEAT TREATED AT 1850 F FOR 5 MIN AFTER PRESSURE BONDING

No core-to-cladding reaction can be observed. Crystalline carbon coating on the core was 15 to 40  $\mu$  in. thick.



250X

RM13925

FIGURE 13. AREA IN AN AS-PRESSURE-BONDED FUEL ELEMENT SIMILAR TO THAT SHOWN IN FIGURE 11 EXCEPT REVEALING POSSIBLE SLIGHT CORE-TO-CLADDING REACTION

The zone of blank structure of the Zircaloy adjacent to the core was interpreted as an indication that the zone had a high oxygen content as a result of core-to-cladding reaction. Such areas were infrequently observed in elements containing cores with these 15 to 40- $\mu$ in. -thick coatings of crystalline carbon. Note the good Zircaloy-to-Zircaloy bond.

A fuel element was pressure bonded containing cores which had not been sand-blasted prior to coating and onto which crystalline-carbon coatings only 1  $\mu$ in. thick had been applied, since thicker pyrolytic carbon coatings were found not to be adherent to cores with as-sintered surfaces. Sections of this element were examined metallographically to determine if these very thin coatings would be sufficiently adherent not to adversely affect the Zircaloy-to-Zircaloy bonding in the element. It was observed that extensive reaction occurred between the core and the cladding during pressure bonding; a 0.001-in.-wide zone of uranium-zirconium reaction products was visible around each of the cores. This specimen was comparable in metallographic appearance to ones containing bare uranium dioxide cores, as shown in BMI-1374.<sup>(2)</sup> The Zircaloy-to-Zircaloy bonds in the element were of high quality, however.

No core-to-cladding reaction occurred during pressure bonding at 1525 F of chromium-coated cores, and no appreciable diffusion of the chromium barrier into the Zircaloy was observed, as shown in Figure 14. Part of the chromium layer was not removed during polishing and etching and is visible in this photomicrograph. The chromium layer is more readily observed in Figure 15, which shows at a higher magnification an area at the corner of a chromium-coated core is an unetched sample. Examination of these specimens containing cores with 25 to 100- $\mu$ in.-thick chromium coatings after a postbonding heat treatment at 1850 F for 5 min revealed that no apparent core-to-cladding reaction occurred, but that diffusion of chromium from the barrier layer into the Zircaloy cladding did take place. The resulting narrow zone of chromium-rich Zircaloy surrounding the cores in these elements did not affect their normally good corrosion behavior, however, based on the results presented later in this report. A fuel element containing cores coated with chromium only 5 to 10  $\mu$ in. thick showed evidence of some core-to-cladding reaction in most areas in most areas in both the as-bonded and as-heat-treated conditions. These areas in the as-bonded condition were similar in appearance to that shown in Figure 13. Portions of this element which were in each condition also showed slight growth during corrosion testing of defected compartments, as reported in a later section, demonstrating that these thinner coatings were not satisfactory to prevent core-to-cladding reaction. Most of the chromium-coated cores used in this study had coatings that were 25 to 40  $\mu$ in. thick which consistently yielded satisfactory results. As expected, the Zircaloy-to-Zircaloy bonds in the elements containing chromium-coated cores were consistently good.

Graphite-coated cores were also found not to react with the Zircaloy cladding during pressure bonding or subsequent heat treatment, except for slight apparent reaction occasionally at the corner of a core. The sprayed, outgassed, and buffed coatings of graphite were applied in all cases in the amount of approximately 5 mg of graphite after buffing per in.<sup>2</sup> of core surface. A typical area of an interface between a Zircaloy cladding plate and a graphite-coated core is shown in Figure 16 in the as-bonded condition. Normally, no reaction was observed at the corners of these cores in the as-bonded or as-heat-treated conditions, as shown in the photomicrograph in Figure 17 of a heat-treated specimen, but occasionally slight reaction, as illustrated in Figure 13, was observed in these susceptible regions. Such areas of slight reaction were observed more frequently in the case of cores coated with graphite than with the other two coatings; however, they did not occur frequently or have a deleterious effect on the corrosion behavior of the elements.



FIGURE 14. TYPICAL AS-PRESSURE-BONDED INTERFACE BETWEEN A ZIRCALOY CLADDING PLATE AND A URANIUM DIOXIDE CORE COATED WITH 25 TO 40- $\mu$  IN. -THICK CHROMIUM BY VACUUM EVAPORATION

There is no visible core-to-cladding reaction or diffusion of chromium into the Zircaloy. Part of the chromium layer was not removed during polishing and etching and is visible in the photomicrograph.

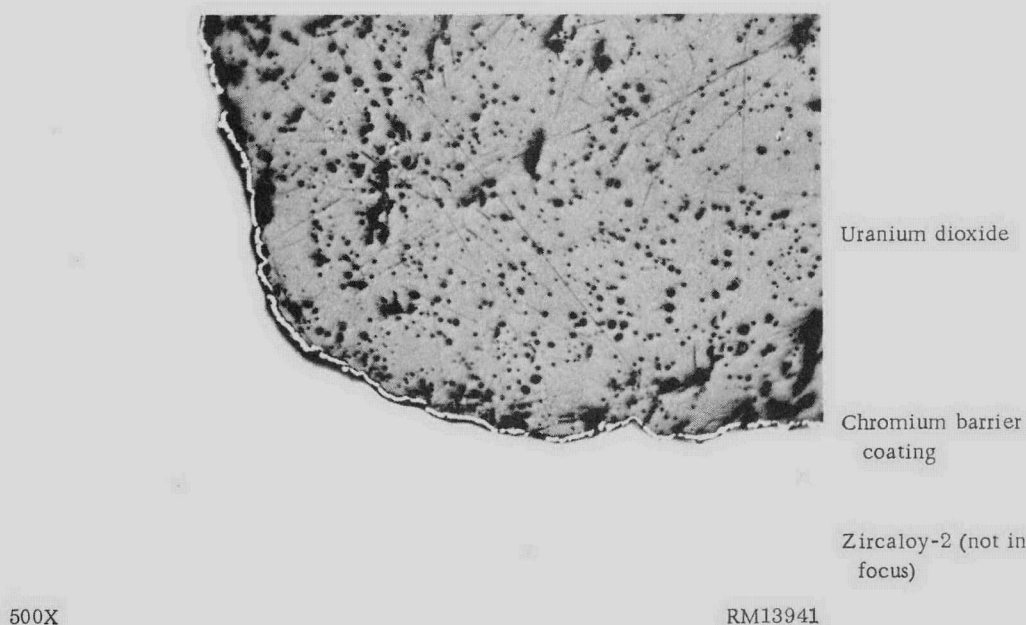


FIGURE 15. AREA AT CORNER OF A CHROMIUM-COATED CORE IN AN UNETCHED SAMPLE SHOWING CHROMIUM COATING

Examination indicated that part of the coating was removed during polishing. The Zircaloy cladding adjacent to the core is not in focus.

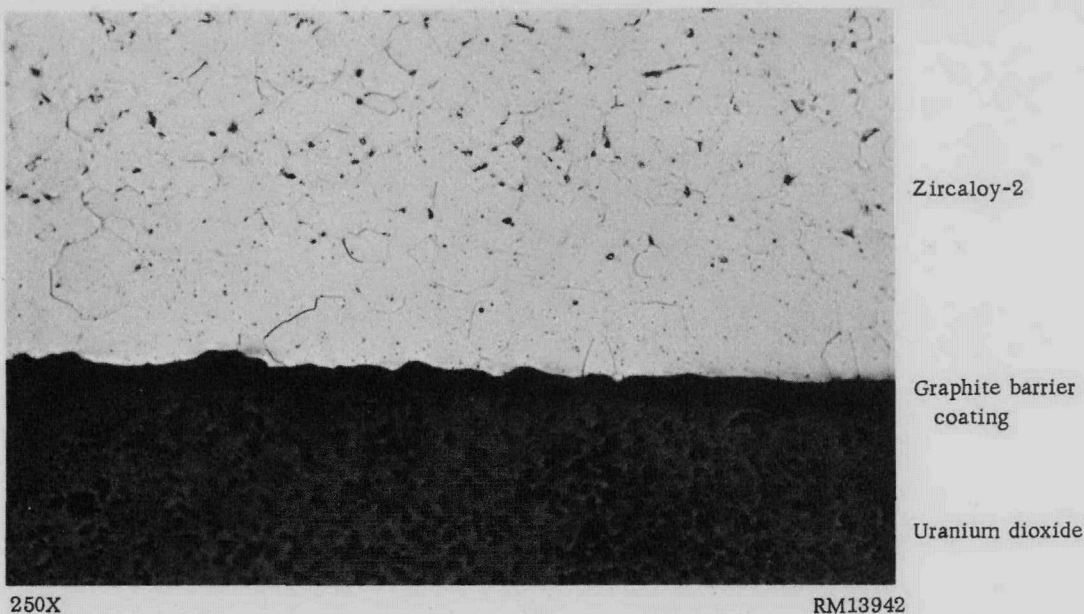


FIGURE 16. TYPICAL AS-PRESSURE-BONDED INTERFACE BETWEEN A ZIRCALOY CLADDING PLATE AND A URANIUM DIOXIDE CORE COATED WITH 5 MG OF BUFFED GRAPHITE PER IN.<sup>2</sup> OF CORE SURFACE

No core-to-cladding reaction occurred.



FIGURE 17. TYPICAL INTERFACE BETWEEN THE ZIRCALOY CLADDING COMPONENTS AND THE CORNER OF A URANIUM DIOXIDE CORE COATED WITH BUFFED GRAPHITE IN A PRESSURE-BONDED AND HEAT-TREATED FUEL ELEMENT

The element was heat treated for 5 min in an 1850 F salt bath. The core was coated with 5 mg of buffed graphite per in.<sup>2</sup> of core surface. This area shows no core-to-cladding reaction; occasionally, similar areas revealed slight reaction. Note excellent Zircaloy-to-Zircaloy bond.

Corrosion and Intercompartmental-Leakage Testing

Corrosion tests were conducted to determine the resistance of purposely defected compartments of the fuel elements to attack in 680 F degassed water. If core-to-cladding reaction occurred, it was indicated by attack at the interface and by swelling of the compartments. These corrosion tests were conducted in conjunction with intercompartmental-leakage tests in order to evaluate the integrity of the bonding between the Zircaloy cladding components before and after corrosion testing. The manner in which the tests were conducted was previously reported.<sup>(2)</sup> In general, the corrosion tests were conducted on compartments with 0.040-in.-diameter defect holes, and the intercompartmental-leakage test consisted of applying 700 psi of helium pressure successively to alternate compartments before and after each corrosion-test interval.

The results of the corrosion and intercompartmental-leakage tests of purposely defected compartments presented in Table 4 demonstrated that the fuel elements showed good corrosion behavior in 680 F water and complete compartment integrity when the cores were properly coated with graphite, crystalline carbon, or chromium. The sprayed, outgassed, and buffed coatings of about 5 mg of graphite per in.<sup>2</sup> of core surface were satisfactory in minimizing core to cladding reaction. It was found that the evaporated chromium coatings must be about 25 to 40  $\mu$ in. thick and that the pyrolytic crystalline-carbon coatings must be about 15 to 40  $\mu$ in. thick in order to satisfactorily minimize the reaction. Slight growth, as indicated in the table, was observed in several isolated compartments in elements containing cores coated with crystalline carbon or chromium during the early stage of the program when these coating techniques were being developed. Since this was not observed in later specimens, it was believed due to some inconsistency in the coatings resulting from changes in procedures during early development of these coating processes, as discussed later. Since none of the specimens with any of the three core coatings showed intercompartmental leakage, it appears that the properly applied coatings do not result in contaminated Zircaloy-to-Zircaloy bonds which would permit communication between compartments before corrosion or as a result of bond-line corrosion attack.

Intercompartmental-leakage tests of all of the fuel elements before and after corrosion testing revealed no communication between any of the compartments. Elements in the as-bonded or heat-treated conditions containing cores properly coated with graphite, crystalline carbon, or chromium showed negligible growth during up to 63 days of exposure in the 680 F pressurized water. The Zircaloy-2 cladding of these fuel elements exhibited good corrosion behavior, and had an adherent, shiny black corrosion film. In order to obtain this good corrosion resistance, it was necessary to clean the surfaces of the elements after pressure bonding and after heat treatment by vapor blasting and then pickling. A pickling treatment alone did not provide adequate cleaning of the Zircaloy. Exposed Zircaloy-to-Zircaloy bonds were not visibly attacked during the corrosion testing of these elements.

The elements containing cores with graphite coatings (5 mg of buffed graphite per in.<sup>2</sup> of core surface) did not show any increase in thickness during the corrosion-testing period employed. These results for the graphite-coated cores were corroborated by similar corrosion tests of as-bonded and of heat-treated elements containing cores similarly coated with graphite which were prepared during a previous program.<sup>(2)</sup> These earlier elements did not grow significantly in 168 days of exposure.

TABLE 4. SUMMARY OF RESULTS OF CORROSION TESTS IN 680 F WATER OF PURPOSELY DEFECTED COMPARTMENTS OF GAS-PRESSURE-BONDED ELEMENTS  
None of the compartments revealed any intercompartmental leakage before or after corrosion testing.

Core Coating	Postbonding Heat- Treatment Temperature, F	Number of Elements Tested	Total Number of Compartments Tested	Total Exposure Time in 680 F Water, days	Number of Compartments Showing Growth	Total Growth in Thickness of Compartments, mils
Graphite <sup>(a)</sup>	None	6	40	63	0	0
	1850	2	16	63	0	0
Graphite	None	4	48	56	0	0
	1850	3	32	56	0	0
Graphite	None	3	48	49	0	0
Crystalline carbon (>15 $\mu$ in.)	None	2	12	63	1	6
	1850	2	12	63	0	0
Crystalline carbon (>15 $\mu$ in.)	None	3	36	56	3	2-5
	1850	1	12	56	1	4
Crystalline carbon (>15 $\mu$ in.)	None	5	80	49	0	0
Crystalline carbon (1 $\mu$ in.) <sup>(b)</sup>	None	1	16	35	16	2-7
Chromium (5-10 $\mu$ in.)	None	1	8	49	3	2
	1850	1	8	63	8	2-5
Chromium (>25 $\mu$ in.)	None	1	8	63	0	0
	1850	1	8	63	0	0
Chromium (>25 $\mu$ in.)	None	2	24	56	0	0
	1850	1	8	56	6	2
Chromium (>25 $\mu$ in.)	None	3	48	49	0	0
Chromium (>25 $\mu$ in.) <sup>(c)</sup>	None	2	32	49	0	0

(a) All graphite coatings were sprayed, outgassed, and buffed in the amount of 5 mg of graphite per in.<sup>2</sup> of core surface.

(b) Crystalline-carbon coatings only 1  $\mu$  in. thick were deposited on cores which, unlike those in other specimens, had not been sandblasted.

(c) Chromium coatings were deposited on cores, which unlike those in other specimens, had not been sandblasted.

Specimens in the as-bonded and heat-treated conditions containing cores with properly applied chromium coatings 25 to 100  $\mu$ in. thick or with properly applied crystalline-carbon coatings 15 to 40  $\mu$ in. thick showed no significant growth during corrosion testing. Chromium coatings 5 to 10  $\mu$ in. thick were apparently not sufficient to prevent completely the core-to-cladding reaction, and slight growth of compartments containing cores with these coatings was produced during the corrosion exposure, especially of the heat-treated specimen. An as-bonded element containing cores with the thinner crystalline-carbon coatings (about 1  $\mu$ in. thick) applied on unblasted surfaces showed considerable growth after exposure.

As noted above, it was observed during the corrosion tests that slight growth, as indicated in the table, had occurred in isolated compartments of several different elements prepared early in the program, which may have been due to improperly applied coatings or some other variable. In these isolated instances of growth, it was observed that the increase in thickness occurred during the first week of exposure. From these results, it is apparent that the coating thickness should not be minimized but should be in the range of 25 to 100  $\mu$ in. for chromium and 15 to 40  $\mu$ in. for crystalline carbon.

#### Results of Burst Tests

Numerous burst tests of compartments in the fuel elements prepared for this study were conducted by the procedures previously reported<sup>(2)</sup> in order to evaluate the strength of the Zircaloy-to-Zircaloy bonds and the strength and ductility of the cladding for the different coatings studied. The results of these tests are contained in Table 5. In the total of 166 tests conducted of compartments in all of the elements, failure in all cases involved rupture of the cladding plates at high pressures and normal amounts of deflection, rather than separation of the bonds. These burst tests included 36 tests of compartments containing cores with sprayed and buffed coatings of graphite, 62 tests of compartments containing cores having pyrolytic crystalline-carbon coatings, and 68 tests of compartments containing cores with coatings of vacuum-evaporated chromium.

Since no bond failures were encountered in any of the burst tests, it was indicated that all three types of coatings were equally satisfactory and had no deleterious effect on the Zircaloy-to-Zircaloy bonds in the elements. As can be noted in the table, the cladding of the fuel elements with various types of core coatings failed generally at similar pressures and deflections, indicating the three coatings to be equivalent in preventing embrittlement or weakening of the cladding. The earlier elements prepared in the study were burst tested in both the as-bonded and heat-treated conditions. The results of the tests with regard to cladding strength and ductility were comparable for both conditions, and no bond failures were encountered in elements in either condition. On the basis of the results of these tests and of other tests discussed later, the post-bonding heat treatment at 1850 F was eliminated from the bonding process, and subsequent fuel elements were evaluated only in the as-bonded condition.

Included in Table 5 are the results of burst tests of 12 compartments in several as-bonded fuel elements which contained cores that were not sandblasted prior to application of coatings of evaporated chromium or pyrolytic carbon. As discussed previously,

TABLE 5. RESULTS OF BURST TESTS OF FUEL ELEMENTS BONDED AT 1525 OR 1550 F AND 10,000 PSI FOR 4 HR

All 166 burst tests of these elements resulted in rupture of the cladding material, rather than in failure of a Zircaloy-to-Zircaloy bond.

Condition Tested	Core Coating	Number of Compartments Tested	Average Burst Pressure, psi	Average Cladding Deflection, mils		
				Area of Burst	Area Adjacent to Burst	Measured at Gage Hole
As bonded <sup>(a)</sup>	Graphite	28	3800	40	34	15
Beta treated <sup>(b)</sup>	Graphite	8	5300	61	60	31
As bonded <sup>(c)</sup>	Chromium	48	4200	32	27	17
Beta treated <sup>(d)</sup>	Chromium	12	5000	59	55	30
As bonded <sup>(e)</sup>	Chromium	8	3700	30	24	17
As bonded <sup>(a)</sup>	Crystalline carbon	48	4800	43	34	15
Beta treated <sup>(d)</sup>	Crystalline carbon	4	6100	61	57	25
As bonded <sup>(a)</sup>	Crystalline carbon <sup>(f)</sup>	4	5100	40	32	16
As bonded <sup>(a)</sup>	Crystalline carbon <sup>(g)</sup>	6	4900	35	26	15

(a) Specimens bonded 4 hr at 1550 F at 10,000 psi with a coating of sprayed and buffed graphite 5 mg per in.<sup>2</sup> thick.

(b) Specimens identical to (a) except they were given an additional treatment at 1850 F for 5 min.

(c) Specimens bonded at 1525 F for 4 hr at 10,000 psi with a 40 to 100- $\mu$ in. coating of chromium.

(d) Specimens identical to (c) except they were given an additional treatment at 1850 F for 5 min.

(e) Specimens bonded at 1525 F at 10,000 psi for 4 hr with 40 to 100- $\mu$ in. coatings of chromium on cores which had not been sandblasted.

(f) Specimens bonded as in (a) with crystalline-carbon coatings 1  $\mu$ in. thick on cores which had not been sandblasted.

(g) Specimens bonded as in (a) with an attempt made during assembly to smear the crystalline-carbon coatings onto the Zircaloy bonding surfaces.

most of the cores coated with pyrolytic crystalline carbon or evaporated chromium had been sandblasted to obtain the optimum condition for adherency of the coating. However, the results of the burst tests indicated that the coatings of chromium applied to cores in the as-sintered condition had satisfactory adherence. Therefore, it was concluded that the sandblasting treatment was not necessary prior to the application of coatings of vacuum-evaporated chromium. In order to apply adherent coatings of pyrolytic crystalline carbon to unblasted cores, however, it was necessary to reduce the thickness of the coating from about 15 to 40  $\mu$ in. to about 1  $\mu$ in. The burst tests listed in the table of an element containing these cores indicated that the thick, pyrolytic carbon coatings were adherent and did not result in contamination and weakening of the bonds; however, these thinner pyrolytic carbon coatings were not effective in preventing core-to-cladding reaction, as discussed previously.

The previously described fuel element containing sandblasted cores coated with crystalline carbon which was purposely mishandled during assembly to determine if these coatings could be smeared onto bonding surfaces and affect bonding was also burst tested. Six burst tests of this element, listed in the table, did not result in any bond failures, indicating that normal handling during assembly of cores which have been sandblasted and coated with pyrolytic carbon probably will not result in poor bonding.

#### Results of Chemical Analyses of the Cladding

The Zircaloy cladding was analyzed after bonding to determine if the cladding had become contaminated by the core coating or if the coating was not effective in preventing core-to-cladding reaction. Portions of cladding were removed from pressure-bonded fuel elements, cleaned, and analyzed. The results were compared with the analyses of the original cladding material. The analyses were of cladding from elements in the as-pressure-bonded condition, since it had been found prior to the time these determinations were made that the postbonding heat treatment at 1850 F for 5 min was not necessary in the process. The cladding from elements with the crystalline-carbon and graphite core coatings was analyzed for carbon to determine if the cladding had been contaminated by the diffusion of carbon during bonding. The results were all comparable to the original material, indicating that no carbon contamination had occurred in the body of the cladding plates. The compositions of cladding samples of as-pressure-bonded elements having chromium-coated cores were also determined, and the analyses revealed no appreciable diffusion of chromium into the cladding. Similarly prepared samples of the cladding removed from pressure-bonded elements containing each of three core coatings were analyzed for uranium to determine if any core-to-cladding reaction and subsequent diffusion of the uranium into the Zircaloy cladding had occurred. The analyses showed that there was no significant amount of uranium in the cladding after bonding.

Vacuum-fusion analyses for oxygen and hydrogen were performed on samples of the Zircaloy cladding plates from pressure-bonded fuel elements with the three types of core coatings. The results of these analyses and analyses of the base material are listed in Table 6. The data show that there does not appear to be any serious problem with regard to contamination of the Zircaloy cladding with oxygen or hydrogen during pressure bonding.

TABLE 6. VACUUM-FUSION ANALYSES OF ZIRCALOY CLADDING  
FOR OXYGEN AND HYDROGEN

The samples of Zircaloy cladding were removed from fuel elements which had been gas-pressure bonded at 1525 F and 10,000 psi for 4 hr.

Coating on Cores of Element	Analysis, ppm	
	Oxygen	Hydrogen
As-received material	1290	29
Crystalline carbon	1390	23
Graphite	1470	49
	1720	41
	1390	31
Chromium	1200	40

Study of Flow of Cladding During Gas-Pressure Bonding Into Void Spaces  
In Picture Frames of Fuel Elements

A problem which was encountered in gas-pressure-bonded fuel elements during the previous program was the occurrence of severe localized depressions and thinning of the cladding due to flow of the cladding-plate material during bonding into void spaces in the picture-frame assembly.(2) These void spaces were present due to chipped cores and other inadvertent internal void regions resulting from assembly tolerances. During gas-pressure bonding, the Zircaloy cladding flowed into these regions, filling all void space, which produced the cladding depressions and thinning. In cases of extensive flow into some shapes and sizes of void space, the cladding plates were ruptured, or the graphite barrier layers being employed were removed from the cores in the regions of excessive flow, thus permitting core-to-cladding reaction.

The elements prepared in the previous program contained several uranium dioxide platelets in each compartment, and it was usually observed that the depressions and thinning were severe only when essentially all of the void was filled by excessive flow of the cladding plates. In the present program, therefore, the cores were individually compartmentalized by Zircaloy ribs in order to determine if it was feasible to minimize excessive flow of the cladding plates into voids by this technique. This design also offers maximum restriction of any cladding failure occurring during service of the fuel element. Although this configuration necessitated the use of additional Zircaloy ribs, the amount of Zircaloy contained in the picture-frame assembly was maintained constant by slightly decreasing the width of all of the Zircaloy ribs for this program to 0.035 in., as compared with the width of 0.040 in. used in the previous program.(2)

It was desired to determine the maximum amount of void space which could be tolerated using this design without resulting in excessive thinning of the cladding or excessive core-to-cladding reaction. To study this effect, specimens were assembled having intentional void spaces of controlled geometry and size. Several of these specimens were bonded in protective containers(2, 9) to determine the effect of the container

and accompanying Ti-Namel spacers on the amount of flow into a given void space, as compared with the edge-welded specimen. It was considered in the evaluation of the results of this study that depressions up to 10 mils in the cladding surface were permissible if they were not accompanied by any significant thinning of the cladding plates.

For this study, nine specimens were prepared in sets of three. Two sets were prepared by the edge-welding technique and had, respectively, graphite-coated and crystalline-carbon-coated cores. The three elements of the third set contained graphite-coated cores and were each assembled with accompanying spacers into a protective container for bonding. One of the three elements in each set was assembled with the minimum possible internal void space, the second contained various measured amounts of void space at the end of each longitudinal row of compartmented cores to simulate poor dimensional control, and the third contained cores from which various measured amounts of material had been ground from one corner to simulate chipped cores. The desired amount of longitudinal void space was obtained by using different sizes of shims at the ends of the various rows of cores.

These specimens were sectioned and evaluated in both the as-bonded and heat-treated conditions. The amounts of intentional void space at the ends of the four longitudinal rows of cores on each size of the element were 0, 10, 20, and 35 mils, arranged as shown in Figure 18.

The simulated chips ground from the corners of the cores were the shape of a regular triangular prism with the altitude being the thickness of the cores. The sizes of simulated chips studied were 10, 25, 50, and 75 mils as a side of the equilateral triangle. These defected cores were arranged in the elements as shown in Figure 19.

The evaluation of the specimens with regard to flow into voids was based principally on visual examination of the surfaces of the elements and on metallographic examination of sections removed from the areas of the original void spaces. Measurements were made of the metallographic samples to determine the extent of thinning of the cladding and the depth of the depressions, and observations were made as to the flow patterns and for any evidence of core-to-cladding reaction. The elements were also evaluated by burst tests and by corrosion tests of purposely defected compartments

#### Results of Visual Examination

Visual examination of the elements showed that even the largest amounts of void space of either type did not result in rupture of the cladding due to excessive thinning. This indicated that individually compartmentalizing the cores significantly reduced excessive flow into voids, since defects of smaller size when located between two cores not separated by a Zircaloy rib had produced cladding rupture in previously bonded specimens.

The surface appearance of half of each of two edge-welded elements which contained longitudinal void space and individually compartmentalized cores is shown in Figure 20. The area indicated by the dash marks in Figure 20 is shown enlarged in Figure 21. It can be noted in the pictures that the longitudinal rows of cores which

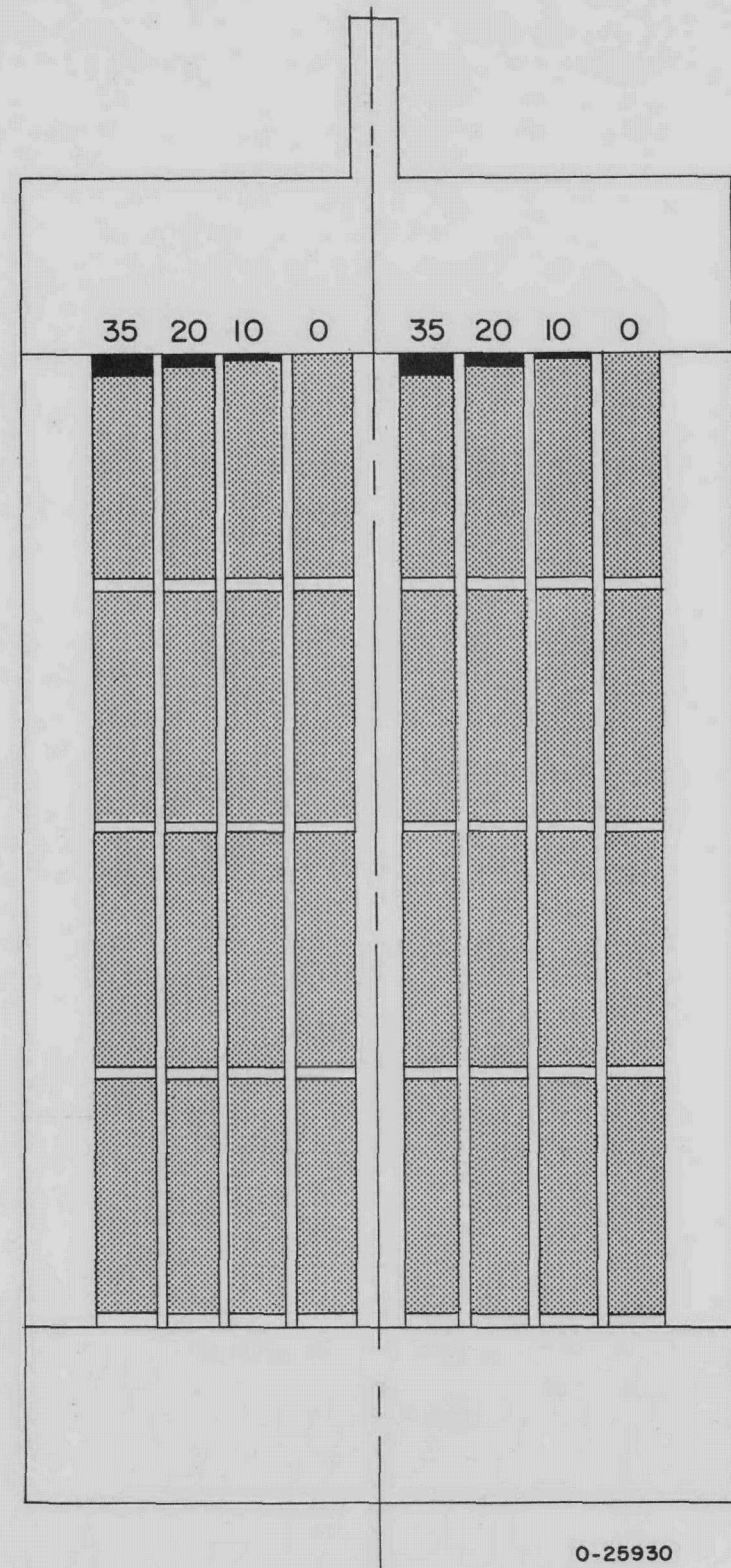


FIGURE 18. DRAWING OF THE ARRANGEMENT OF THE LONGITUDINAL VOID SPACES PURPOSELY INCLUDED IN SEVERAL FUEL ELEMENTS TO STUDY FLOW OF CLADDING DURING GAS-PRESSURE BONDING

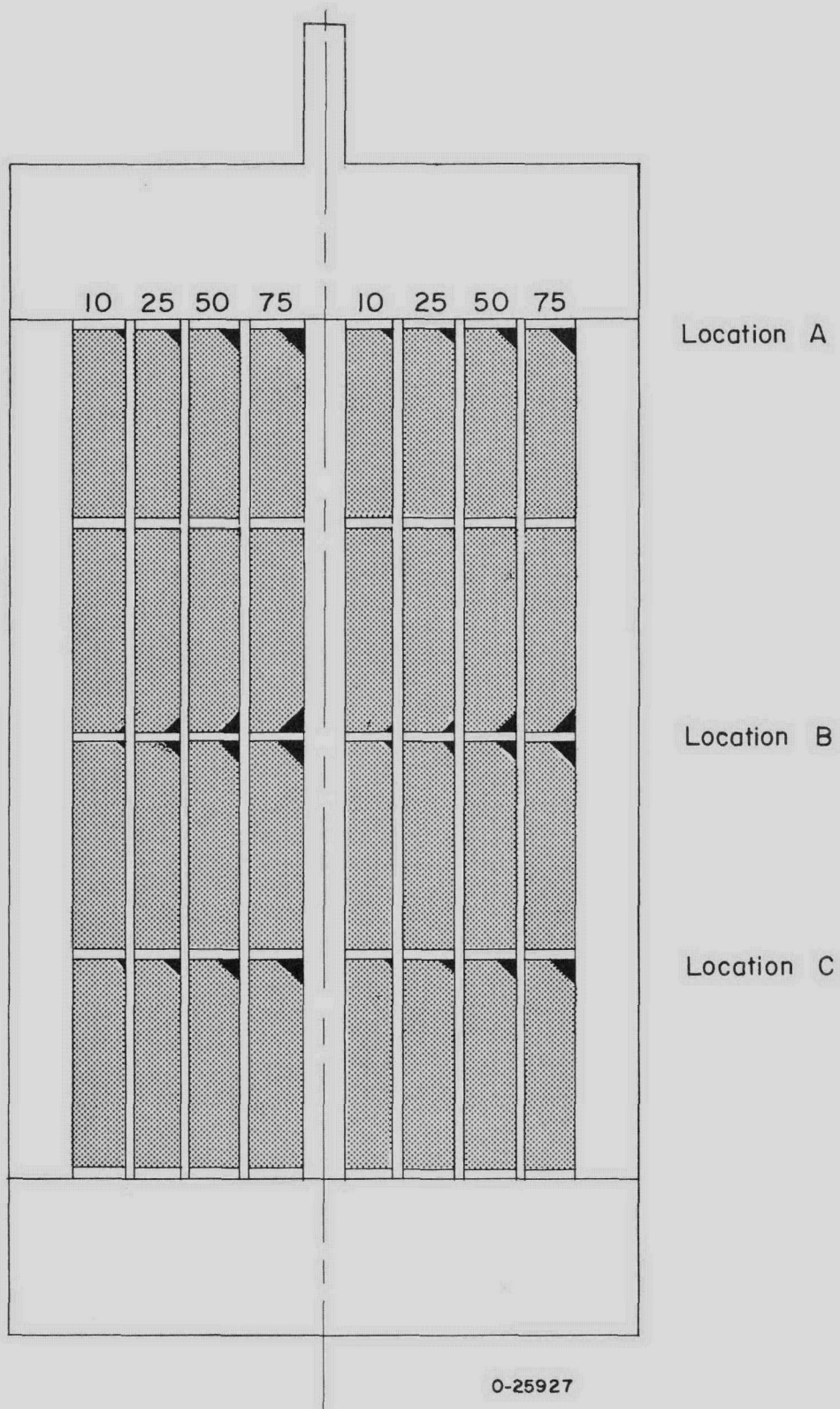


FIGURE 19. DRAWING OF THE ARRANGEMENT OF THE VOID SPACES SIMULATING CHIPPED CORES WHICH WERE INCLUDED IN SEVERAL FUEL ELEMENTS TO STUDY FLOW OF CLADDING

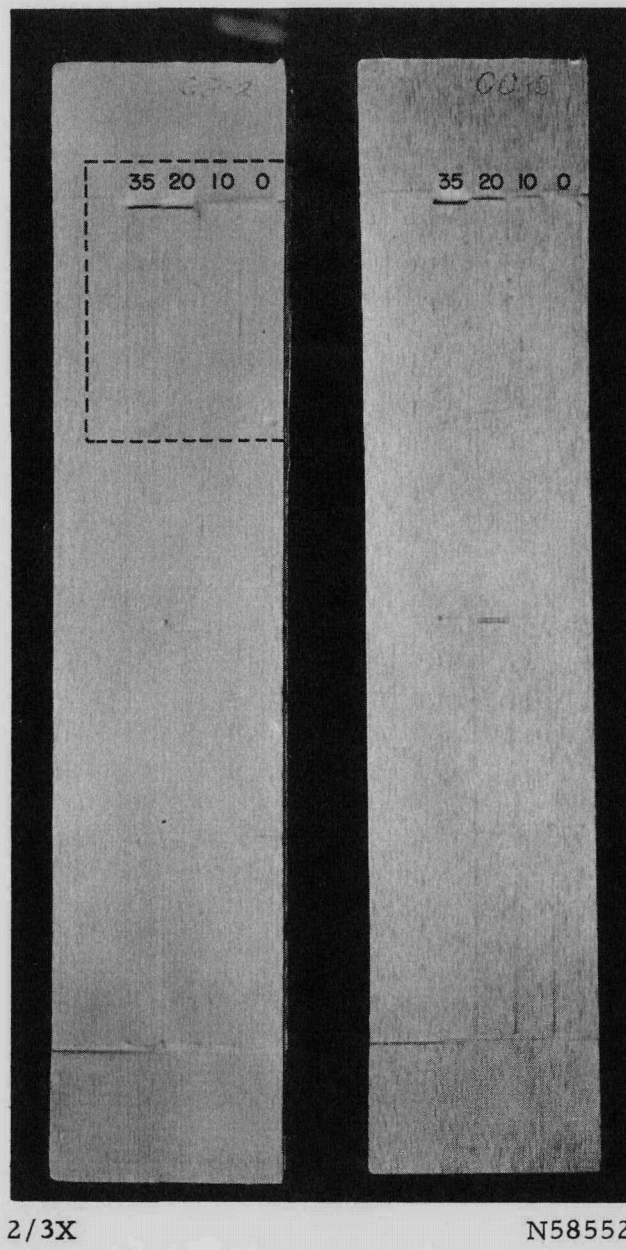
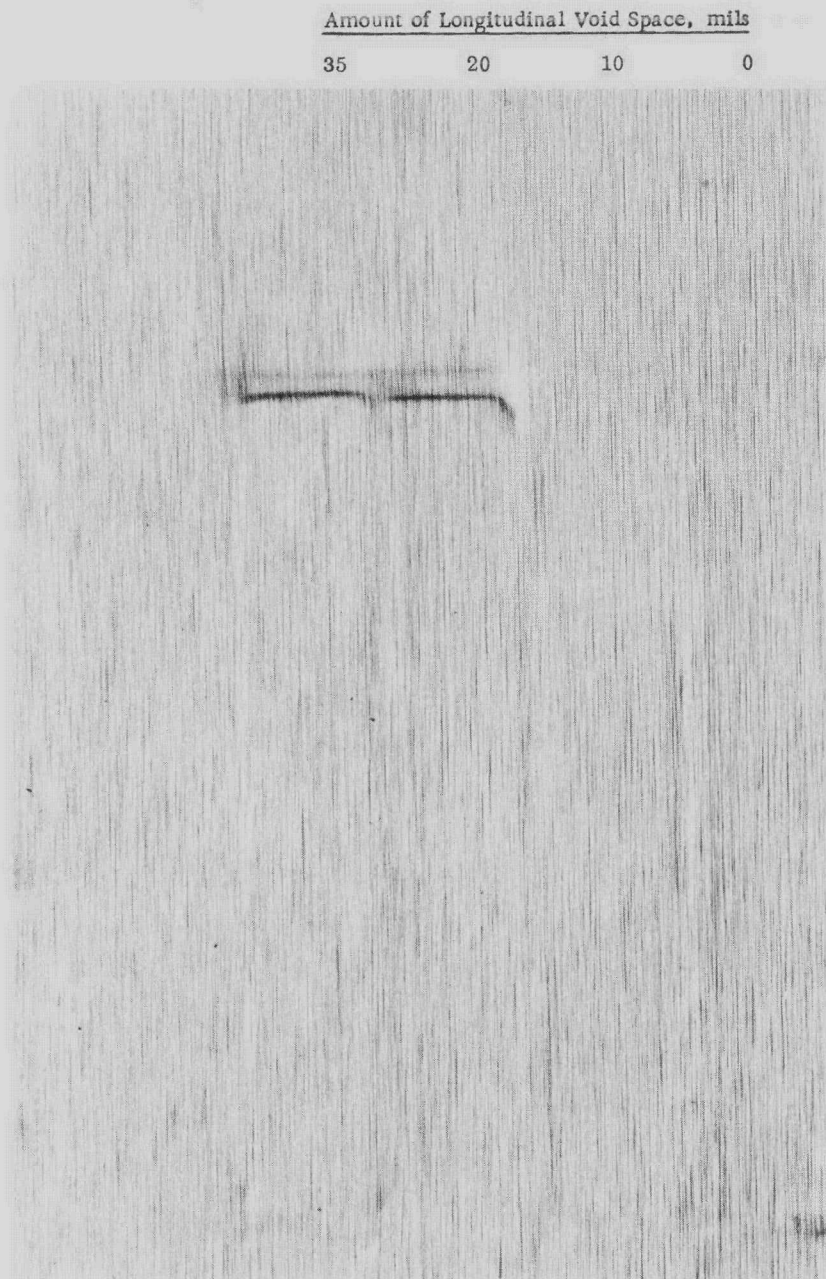


FIGURE 20. APPEARANCE OF THE SURFACES OF EDGE-WELDED AND PRESSURE-BONDED ELEMENTS WHICH CONTAINED INTENTIONAL LONGITUDINAL VOID SPACE

The area indicated by the dash marks is shown at a higher magnification in Figure 21. The amount of void space in mils contained in each of the longitudinal rows of cores is indicated in the photograph. Even with the maximum amount of included void space, no cladding rupture occurred during pressure bonding due to excessive flow.



3X

N58554

FIGURE 21. PHOTOGRAPH SHOWING AT A HIGHER MAGNIFICATION THE AREA INDICATED IN FIGURE 20

The amount of void space contained in each of the longitudinal rows of cores is indicated in the figure.

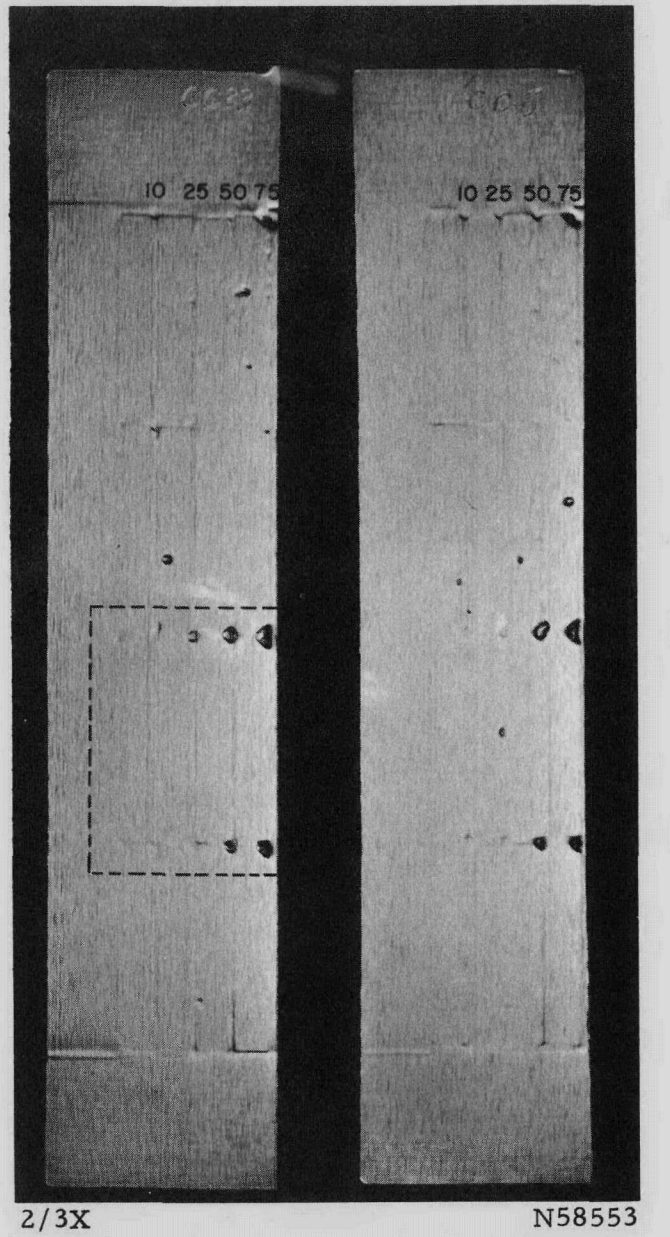


FIGURE 22. APPEARANCE OF THE SURFACE OF EDGE-WELDED AND PRESSURE-BONDED FUEL ELEMENTS WHICH CONTAINED INTENTIONAL VOID SPACES SIMULATING CHIPPED CORES

The area indicated by the dash marks is shown at a higher magnification in Figure 23. The sizes in mils of the simulated chips are indicated in the photograph and described in the text. Even with the maximum amount of included void space, no cladding rupture occurred during pressure bonding due to excessive flow.

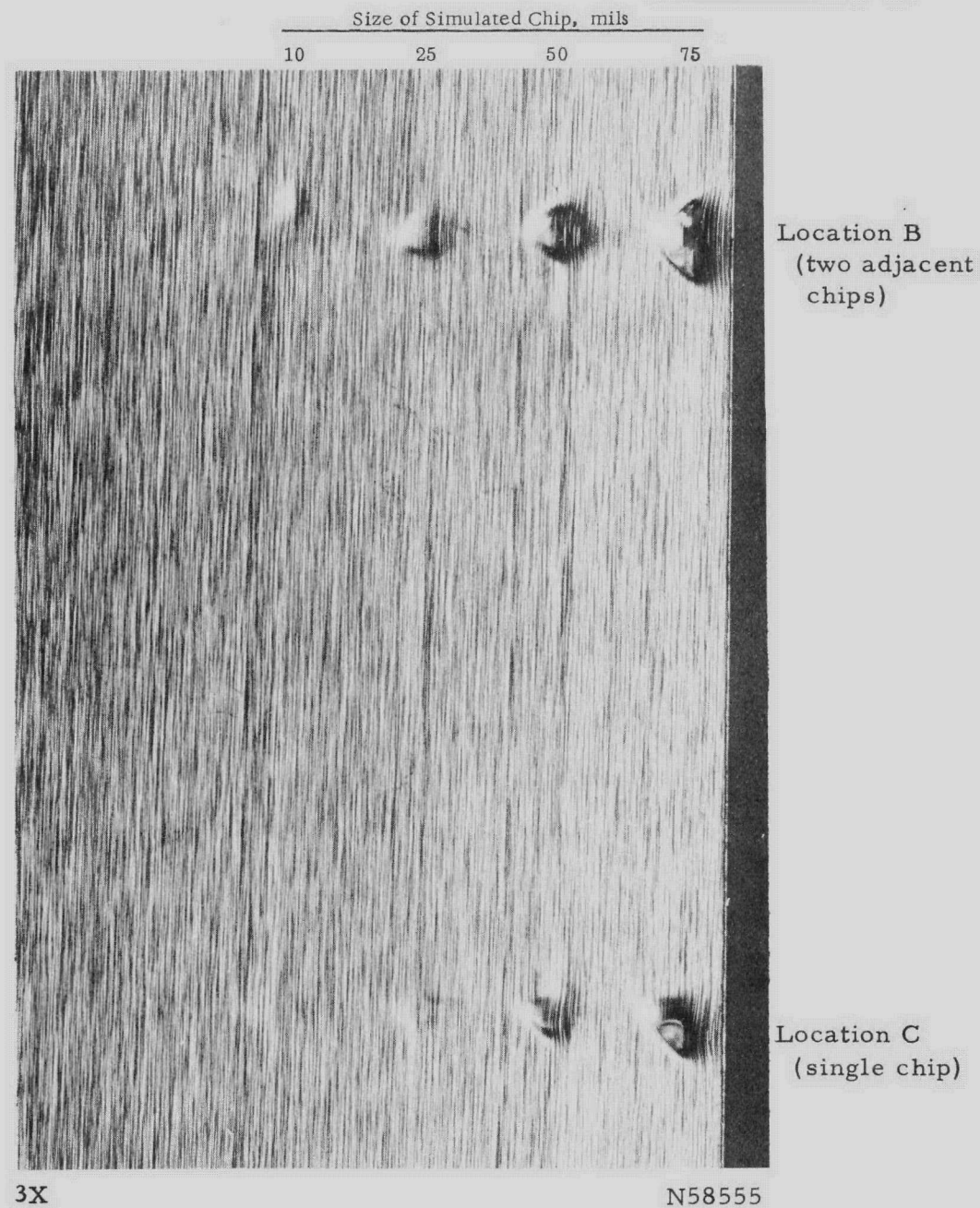


FIGURE 23. AREA INDICATED IN FIGURE 22 BY DASHED LINES AT A HIGHER MAGNIFICATION

The sizes of the simulated chips in the area shown are indicated in the photograph. Locations B and C are indicated in Figure 19.

contained 0 or 10 mils of void space had no visible depressions. It can also be observed in Figure 20 that the longitudinal void space occurred principally at the end of a row of cores corresponding to the top end of the element, which is the numbered end in the photographs. However, radiographs of the elements revealed that the void space was not always concentrated in that location. The slight depression at the center of the longitudinal row of cores which contained 20 mils of void space in the element at the right in Figure 20 apparently resulted from void space which had been present at the location. The elements having longitudinal void space and which were bonded in containers show even smaller depressions than the edge-welded elements, as discussed later.

The surface appearance of edge-welded elements which were bonded containing cores with simulated chips is illustrated in Figure 22. The area indicated by the dashed lines in Figure 22 is shown enlarged in Figure 23. For comparison, the depression at the location of the two adjoining 25-mil simulated chips at the top of Figure 23 is only 5 mils deep. The depressions at the center of the element corresponding to the location of two chips on either side of the transverse Zircaloy rib (as indicated in Figure 19) were, of course, of greater depth than the depressions caused by a single defect of the same size, as can be observed in the photographs. The 10- and 25-mil-size chips, located singly or in pairs, did not result in any deep depressions in the edge-welded elements. The elements containing cores with simulated chips which were bonded with spacers in protective containers showed even shallower depressions than the edge-welded specimens. This can be observed in Figure 24, which shows the same location in an element bonded in a container as is shown in Figure 23 for an edge-welded specimen. In these elements bonded in containers, only the double 75- and 50-mil chips produced deep depressions.

#### Results of Metallographic Examination of Flow

The flow into the intentional voids in the elements was evaluated metallographically by observing the flow patterns, noting any evidence of core-to-cladding reaction, and measuring the depth of the depressions and the minimum thickness of the thinned cladding. Samples were not examined from those locations which had contained the smaller amounts of void space and did not visually show any significant amount of flow. The measurements made of the metallographic samples and observations with regard to core-to-cladding reaction are summarized in Table 7 for the edge-welded elements and elements bonded in containers which contained intentional longitudinal void space. Table 8 contains similar results for the elements which contained cores with simulated chips.

In Table 7, it is shown that a longitudinal void space of 20 mils in edge-welded elements resulted in essentially no thinning of the cladding and only relatively shallow depressions. A void space of 35 mils would not be permissible in edge-welded elements because of the significant depressions and thinning of the cladding. Figure 25 shows the depressions and thinning of the cladding caused by 35 mils of longitudinal void space. The area in the photomicrograph shows the most severe case of flow observed in any location in any of the specimens prepared. The element bonded in a container having longitudinal void space did not show any detrimental effect even from the 35-mil void space.

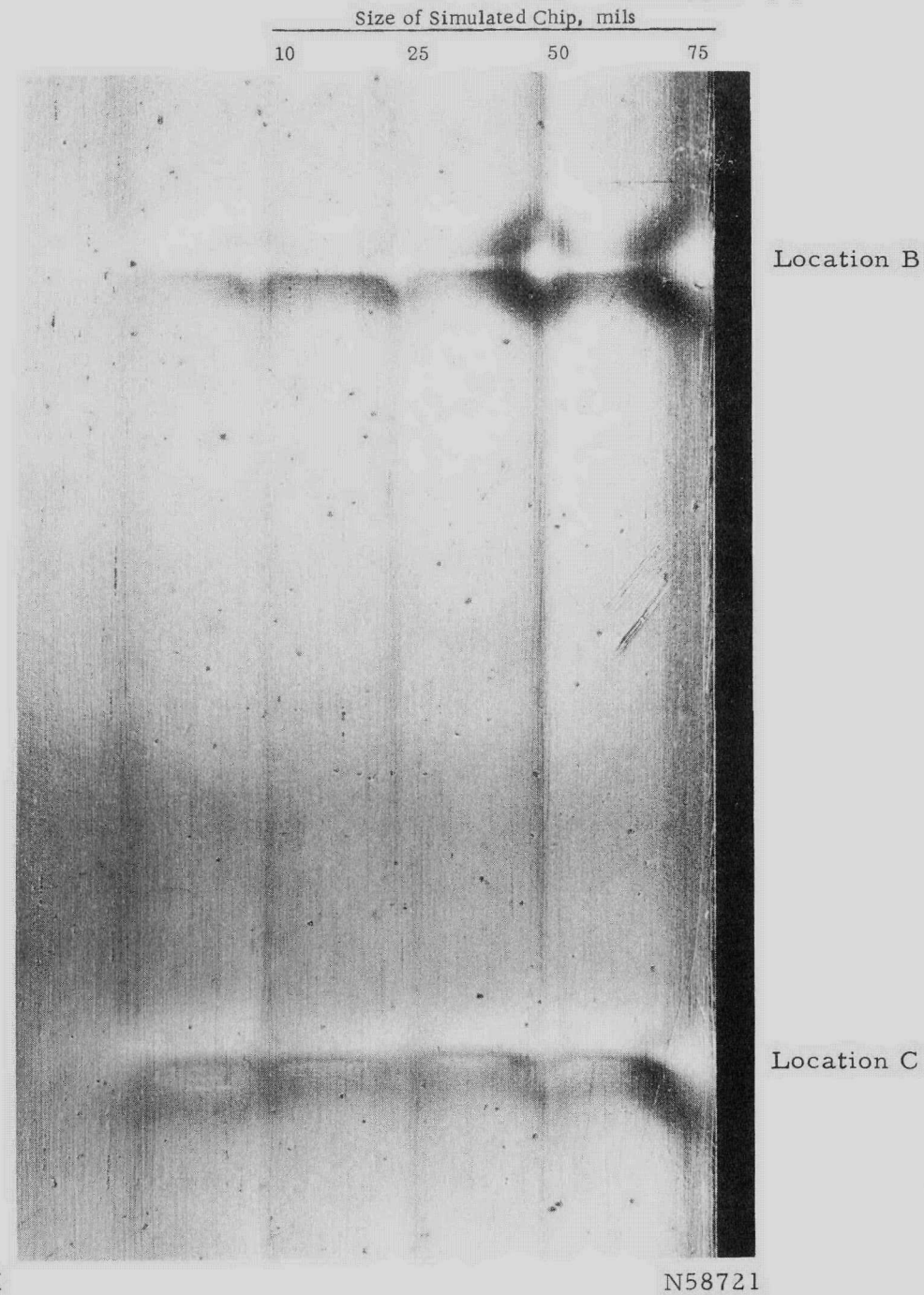


FIGURE 24. SURFACE APPEARANCE OF A FUEL ELEMENT CONTAINING INTENTIONAL VOID SPACES SIMULATING CHIPPED CORES WHICH WAS PRESSURE BONDED IN A PROTECTIVE CONTAINER

This area can be compared with a similar area of an edge-welded specimen shown in Figure 23. The sizes of the simulated chips in the area shown are indicated in the photograph.

TABLE 7. CLADDING DEPRESSION AND THINNING AND CORE-TO-CLADDING REACTION RESULTING FROM LONGITUDINAL VOID SPACE IN CORE ROWS

Locations which had contained 10 mils of longitudinal void space showed no significant amount of flow in edge-welded specimens or specimens bonded in containers.

Amount of Longitudinal Void Space, mils	Type of Specimen	Type of Barrier Layer	Postbonding Heat Treatment	Normal Thickness of Cladding, mils	Minimum Thickness of Cladding at Corner of Core, mils	Maximum Depth of Depression (One Side), mils	Core-to-Cladding Reaction
20	Edge welded	Graphite	None	21.3	21.0	7.0	None
20	Edge welded	Crystalline carbon	1850 F, 5 min	21.6	21.3	6.0	None
35	Container	Graphite	None	21.3	20.4	6.0	None
35	Edge welded	Graphite	1850 F, 5 min	20.7	19.5	15.6	Very slight at one edge of core
35	Edge welded	Crystalline carbon	1850 F, 5 min	20.2	12.6	17.4	None

TABLE 8. CLADDING DEPRESSION AND THINNING AND CORE-TO-CLADDING REACTION RESULTING FROM SIMULATED CHIPPED CORES

Locations which had contained 10-mil chips did not show any significant amount of flow in edge-welded specimens or specimens bonded in containers.

Size of Simulated Chip, mils	Location of Chip <sup>(a)</sup>	Type of Specimen	Type of Barrier Layer	Postbonding Heat Treatment	Normal Thickness of Cladding, mils	Minimum Thickness of Cladding at Corner of Core, mils	Maximum Depth of Depression in Cladding, mils	Core-to-Cladding Reaction
25	B <sup>(b)</sup>	Edge welded	Crystalline carbon	1850 F, 5 min	21.7	20.7	5.0	None
25	C <sup>(c)</sup>	Edge welded	Crystalline carbon	1850 F, 5 min	21.7	21.6	3.6	None
50	B	Container	Graphite	None	21.6	16.6	9.5	Slight reaction at one core
50	C	Edge welded	Crystalline carbon	1850 F, 5 min	21.8	15.0	21.6	None
50	C	Container	Graphite	None	21.8	18.8	5.0	None
75	B	Edge welded	Graphite	None	21.8	11.3	43.8	Slight reaction at corner of one core
75	B	Edge welded	Crystalline carbon	None	22.6	13.3	42.3	Slight reaction at corner of one core
75	B	Container	Graphite	None	21.8	16.5	9.7	Slight reaction at corner of one core
75	C	Edge welded	Crystalline carbon	1850 F, 5 min	22.0	11.5	37.5	None
75	C	Container	Graphite	None	21.0	18.7	5.4	None

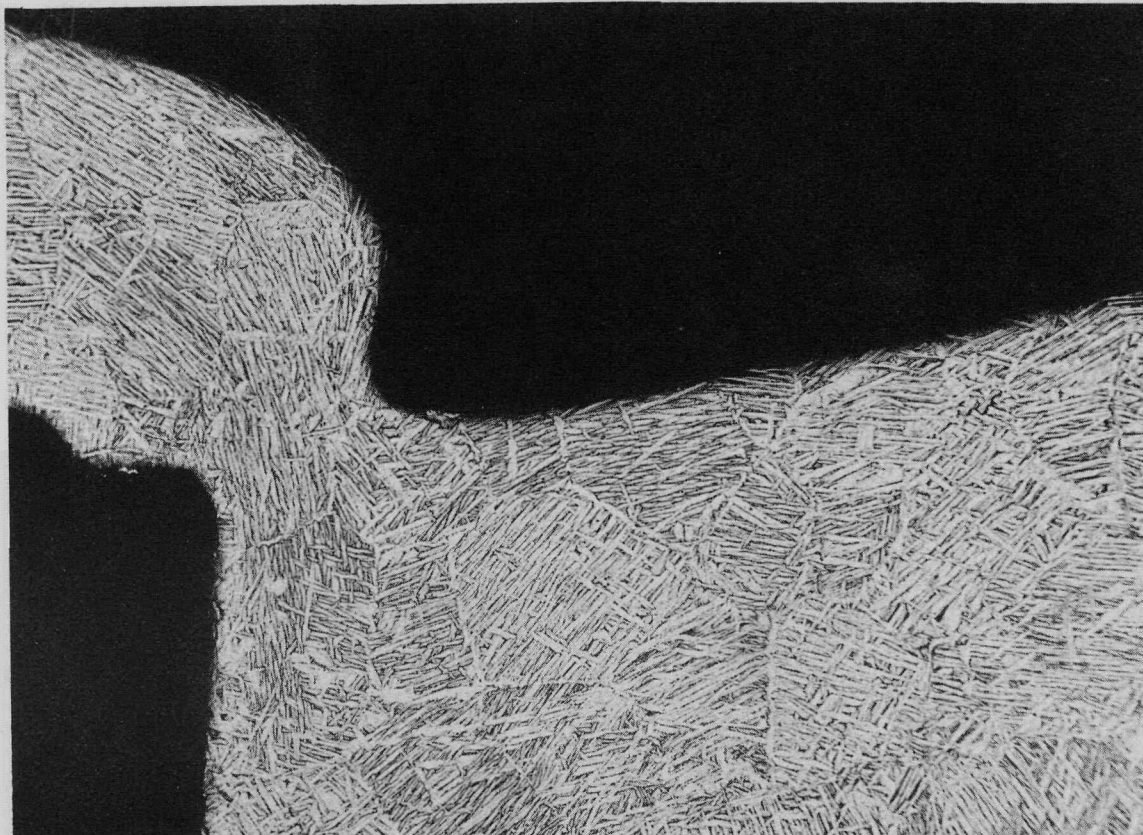
(a) As identified in Figure 19.

(b) Two chips facing center cross rib.

(c) One chip at bottom cross rib.

Zircaloy-2  
cladding plate

Uranium dioxide  
core (removed  
during  
polishing)



Zircaloy-2  
cladding plate

Zircaloy-2  
rib of picture  
frame

RM13121

FIGURE 25. PHOTOMICROGRAPH OF AN AREA SHOWING THE MOST SEVERE FLOW OBSERVED AT ANY LOCATION IN ANY OF THE SPECIMENS PREPARED CONTAINING INTENTIONAL VOID SPACES

Note the depression and thinning of the cladding resulting from excessive flow into the longitudinal void space of 35 mils. The fuel element was of the edge-welded type.

The edge-welded elements containing chipped cores, as listed in Table 8, demonstrated excessive thinning of the cladding and deep depressions in regions where 50- and 75-mil simulated chips had been located singly or in pairs. The specimens bonded in containers generally showed less thinning and less deep depressions than the edge-welded elements for the same size defect, and the effect of 50-mil chips located singly, or, possibly, even in pairs, may not be detrimental.

As indicated in Table 7 and 8, metallographic examination of the samples for evidence of core-to-cladding reaction revealed only small zones of slight reaction at the corners or edges of the graphite-coated and crystalline-carbon-coated cores where the larger voids had been located and maximum flow of the cladding occurred. Thus, even the maximum amount of flow did not result in excessive removal of barrier coatings of either graphite or crystalline carbon. Figure 25 shows a minimum amount of reaction between the cladding and crystalline-carbon-coated core in an area of very severe flow. Several areas of slight reaction between the cladding and graphite-coated cores were observed in the regions of maximum flow. Purposely defected compartments of these elements were corrosion tested in 680 F water to assure that no detrimental effect would be obtained due to the slight reaction observed in some areas. Long-time tests of up to 63 days produced no swelling of the compartments.

The flow patterns in regions of the elements where the voids had been present were studied to obtain a better understanding of the mechanism of flow. Figure 26 shows a region of extensive flow of the cladding plate into a void space in an element bonded in a container. The void space at this location was produced by cores with 75-mil simulated chips placed on either side of the center Zircaloy transverse rib (Location B in Figure 19). The flow patterns were obtained by examination of an etched sample at high magnification and are indicated in the photograph of Figure 26 by dashed lines. It was noted that most of the material to fill the void space flowed into the void region from the longitudinal rib at the side of the region, as indicated in the figure. The transverse Zircaloy rib and the cladding plates had flowed only slightly. Figure 27 shows a similar area in a bonded edge-welded element. Flow of material into the void space occurred primarily from the cladding plates and the transverse rib, which was flattened considerably. Only a small amount of material flowed into the void from the longitudinal rib.

A comparison of the flow occurring in the two types of elements demonstrates the effect of the Ti-Namel spacers on flow in the elements bonded in containers. The spacers apparently tend to distribute evenly and to slow down the flow of the cladding plates, permitting the pressure on the sides of the container to cause considerable flow of the longitudinal ribs. In the edge-welded elements, however, the flow of the cladding plates and the transverse ribs was predominant. It is to be noted, though, that some flow occurred in all directions in both types of elements because of the gas pressure exerted on all sides.

Examination of the effects of flow of the cladding into the void spaces of various size and geometry indicated that a longitudinal void space of 20 mils in edge-welded elements and 35 mils in elements bonded in containers resulted in less than 1 mil of thinning of the cladding and a cladding depression of 7 mils or less. In edge-welded elements, cores with simulated chips of the 25-mil size located singly or in pairs did not result in cladding thinning greater than 1 mil or depressions deeper than 5 mils. In elements bonded with spacers in containers, even the 50- and 75-mil simulated chips

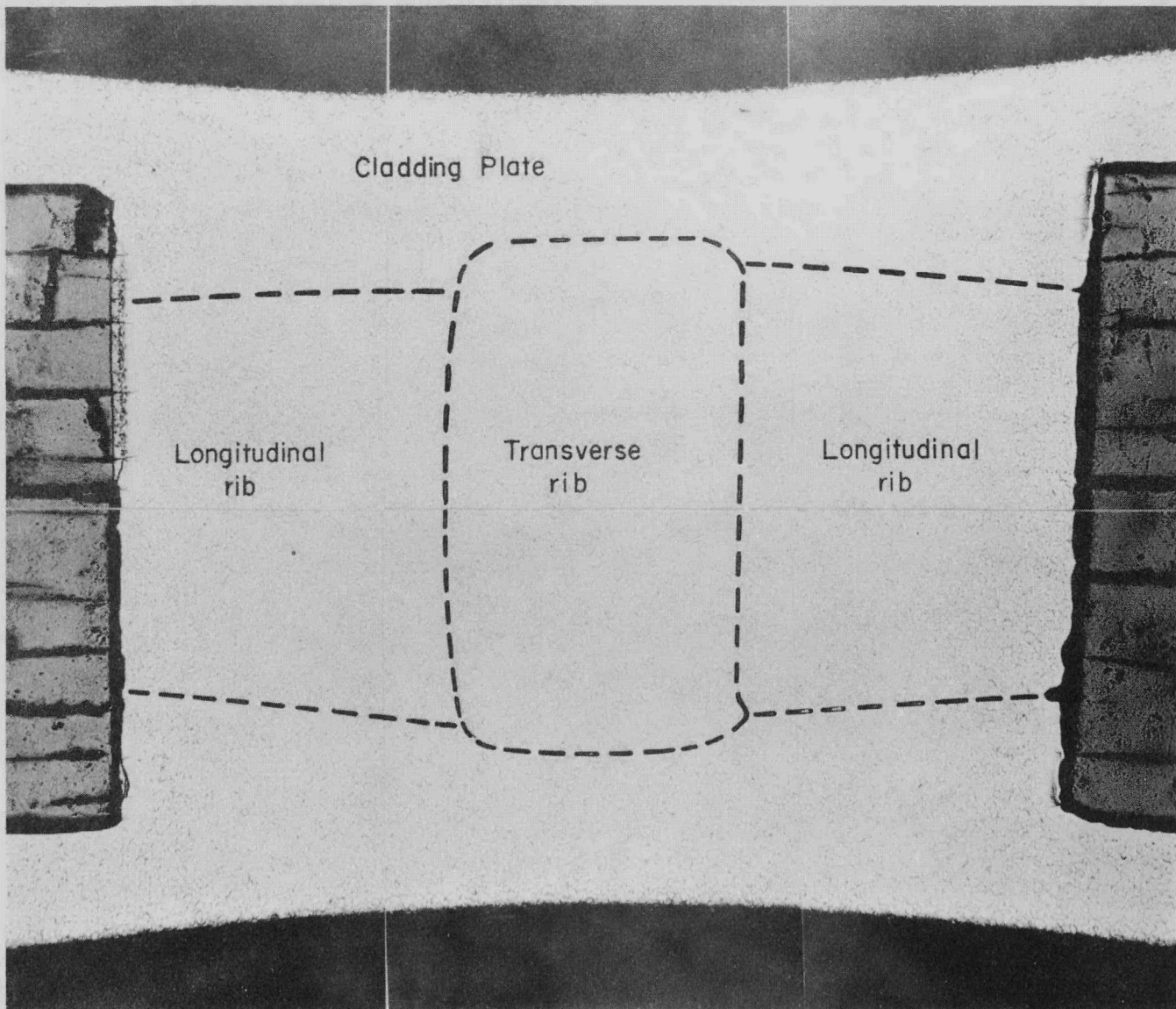
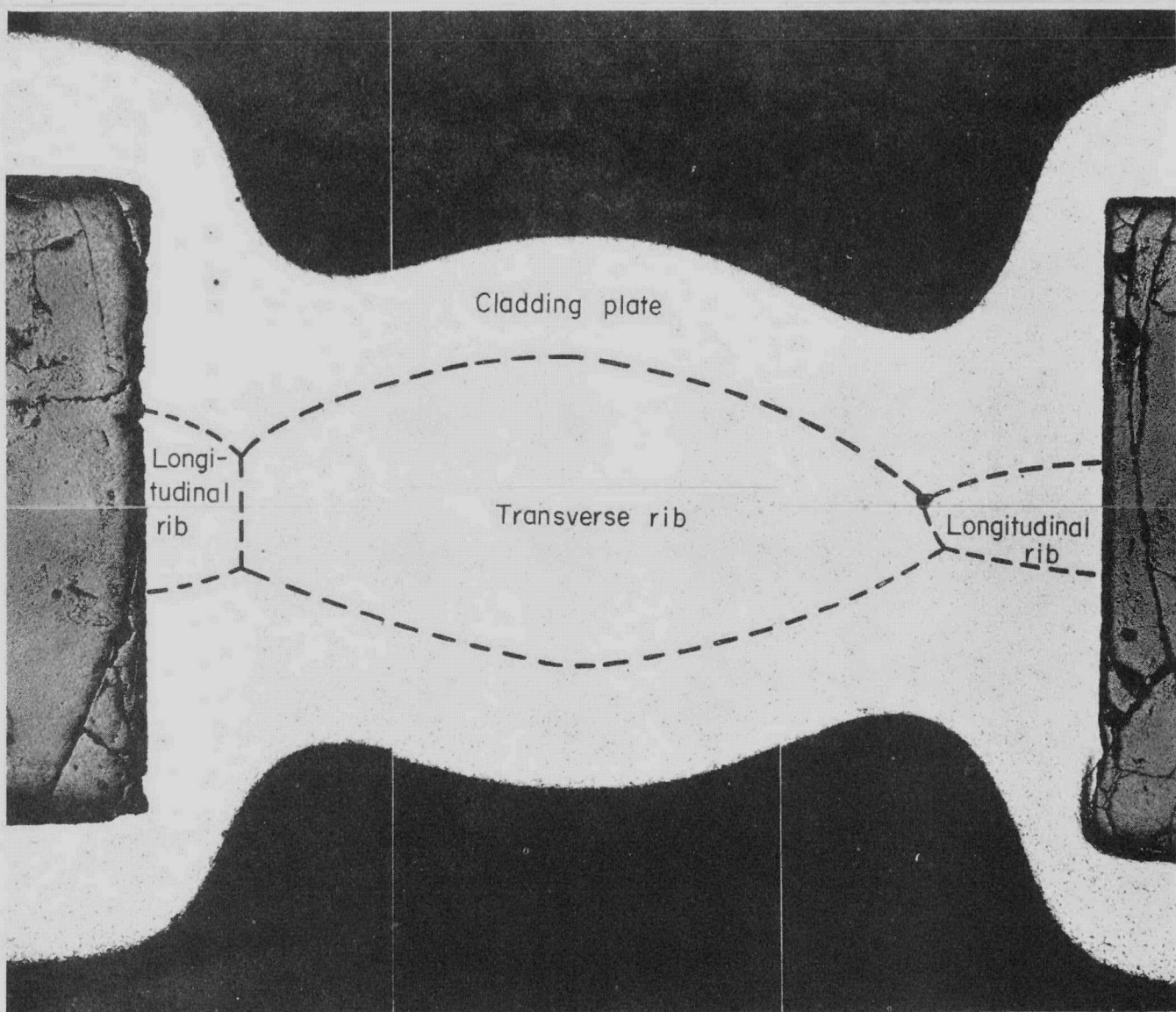


FIGURE 26. PHOTOMICROGRAPH SHOWING FLOW PATTERNS IN A REGION WHICH HAD CONTAINED A LARGE INTENTIONAL VOID SPACE IN A FUEL ELEMENT BONDED IN A PROTECTIVE CONTAINER

The dashed lines outline the regions of the original void space which were filled by flow of the cladding material from the various components indicated. The void space had consisted of two adjacent 75-mil simulated chips in the cores.



40X

N59386

FIGURE 27. FLOW PATTERNS IN A REGION OF AN EDGE-WELDED AND PRESSURE-BONDED FUEL ELEMENT WHICH HAD CONTAINED A LARGE INTENTIONAL VOID SPACE

The dashed lines outline the regions of the original void space which were filled by flow of the cladding material from the various components indicated. Two adjacent 75-mil simulated chips in the cores had formed the void space. This photomicrograph of an edge-welded element can be compared with Figure 26 of an element bonded in a protective container.

located singly did not cause cladding thinning of more than 3 mils or depression of the cladding greater than 6 mils. It was also found during this study that flow of the cladding into the defects did not result in any detrimental removal of the barrier layers of graphite or crystalline carbon nor in excessive subsequent reaction between the core and cladding.

#### Cleaning and Assembly of Specimens for Bonding

The Zircaloy components were cleaned prior to bonding by a process involving degreasing, detergent washing, and rinsing. It was not an objective in this program to attempt to simplify the cleaning procedure, but to follow a standard cycle that seemed to produce clean surfaces. The components were handled with clean rubber gloves or tongs during all operations. The components were degreased by scrubbing in methyl alcohol and then acetone, followed by an ultrasonic degrease (5 min) in warm, pure ethyl alcohol. They were then scrubbed in a hot solution of Alconox, a detergent for metal cleaning, and distilled water. After washing, the components were subjected to a multistep rinsing cycle to insure removal of all of the detergent. They were rinsed by scrubbing in cold distilled water, ultrasonically rinsed (5 min) in warm, pure ethyl alcohol, and then rinsed by dipping in baths of hot, cold, and, again, hot distilled water. Drying of the components was accomplished by blowing them with dry, filtered air, and they were then placed in a dry box prior to assembly. Care was taken to insure that the components did not become dry between operations, which would have left stains on the surfaces. Also, they were not allowed to remain in any of the hot solutions for too long a period of time. The small transverse ribs of the fuel elements were processed through the same cleaning cycle, but the scrubbing operations were performed on groups of ribs in small beakers of the various solutions to expedite scrubbing of the very small components.

Initially in this program, the scrubbing and ultrasonic rinses were not included. These steps were added to the cycle when it appeared that all of the detergent from the washing operation might not have been removed by the rinses involving only dipping. The fuel cores were assembled in the as-coated condition. It was noted during cleaning of the cladding components that it was difficult to remove the Alxonox detergent, which was used in the washing operation, by the rinsing method, which consisted only of dipping the components in several rinsing baths. Since residual Alconox from the cleaning cycle was suspected to be the cause for some of the contaminated bonds, a specimen was prepared with bonding surfaces intentionally contaminated with Alconox. Examination of this specimen after bonding revealed a badly contaminated bond interface, demonstrating that the presence of Alconox had a deleterious effect on bond quality. The contamination along the bond interface and the lack of grain growth as a result of the residual contamination are apparent in Figure 28.

The cycle used in cleaning of components for assembly requires extreme processing care and properly abraded Zircaloy surface to obtain a reasonable consistency of good bonds during subsequent gas-pressure bonding. The cleaning cycle employed for these specimens is being altered and improved by studies being conducted at Bettis and Battelle. Before this process is used in production, proper techniques will be developed to assure that the bonding surfaces are free of contamination that might prevent bonding.

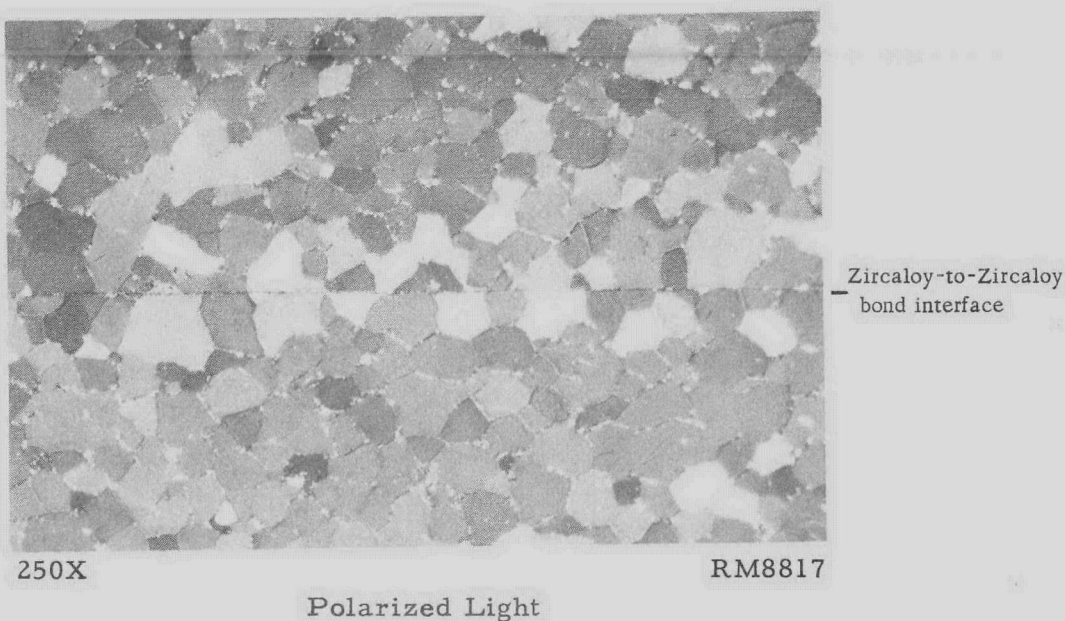


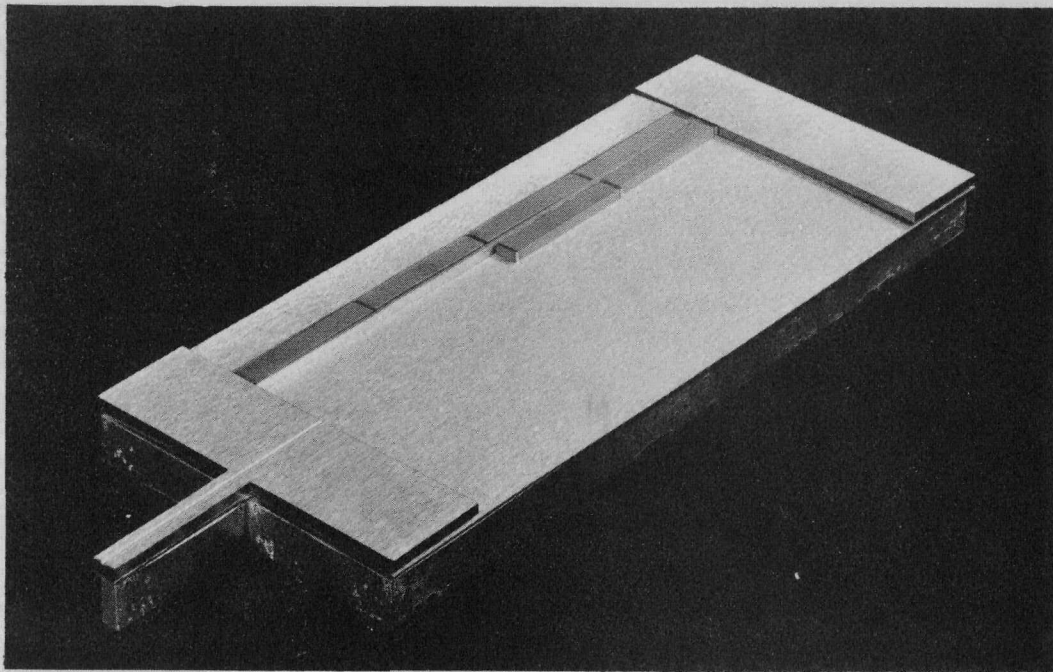
FIGURE 28. POOR ZIRCALOY-TO-ZIRCALOY BOND CONTAMINATED WITH RESIDUAL DETERGENT DUE TO WASHING OF THE ZIRCALOY CLADDING COMPONENTS WITHOUT ADEQUATE RINSING

Improved rinsing operations included in the cleaning of the Zircaloy components for subsequent fuel elements resulted in uncontaminated bonds.

Assembly of the elements was performed using clean rubber gloves. For the elements to be edge welded, the bottom cladding plate was placed on a 0.5-in.-thick copper piece, which had been machined just slightly smaller and the same shape as the element. The copper piece, a duplicate of which was placed on top of the element after assembly, served as a support for the element during assembly and handling and as a cooling block during subsequent edge welding. The picture-frame components and cores were then assembled in position on the cladding plate. Tweezers were used for handling the small transverse ribs. Any residual void space at the end of a longitudinal row of cores was filled using 0.005-in. Zircaloy shims. The assembly of the elements, which was an operation requiring great care, is illustrated in the photographs of Figure 29. The top cladding plate and copper piece were then placed on the assembly. Lateral void space in the picture-frame assembly was removed by pushing inward on the side plates of the frame, and entire assembly was then clamped in position for welding.

Fusion welding of the edges of the cladding plates to the side plates of the picture frame was performed in a helium-atmosphere tank with the element clamped between the copper cooling blocks. Only the end of the evacuation extension was not welded. The elements were then tested to insure that no leaks were present in the welds.

For evacuation and sealing, the evacuation extension of the edge-welded element was connected to a high-vacuum manifold by means of an adapter and a rubber hose, and the element was evacuated for 1 to 2 hr. The extension was then sealed using a resistance-upset welding machine. After disconnecting the element from the evacuation system, the end of the extension was sealed by helium-shielded arc welding to insure

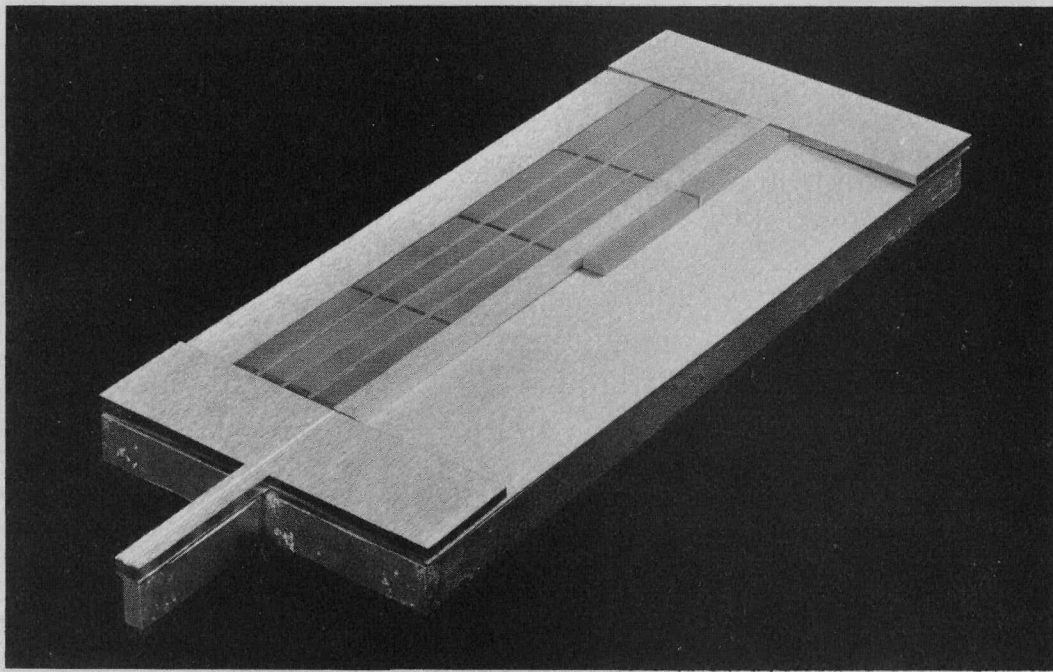


1/2X

N64734

a. Partially Assembled Picture Frame Showing Placement of Zircaloy Cladding Components and Uranium Dioxide Cores

Assembly was performed on one of the cladding plates placed on a copper cooling block which was subsequently used during fusion edge welding of the fuel element.



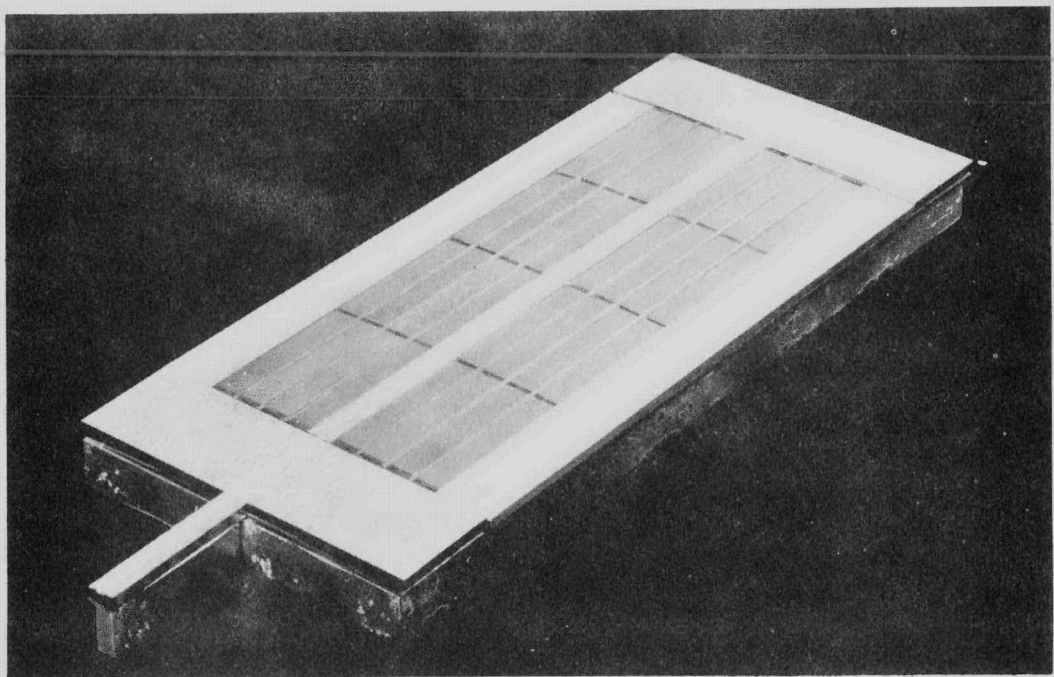
1/2X

N64735

b. Later Stage of Assembly of the Compartmented Picture Frame Containing Uranium Dioxide Cores

Wide Zircaloy plate down the center of the fuel element was utilized to facilitate sectioning of these experimental elements after bonding.

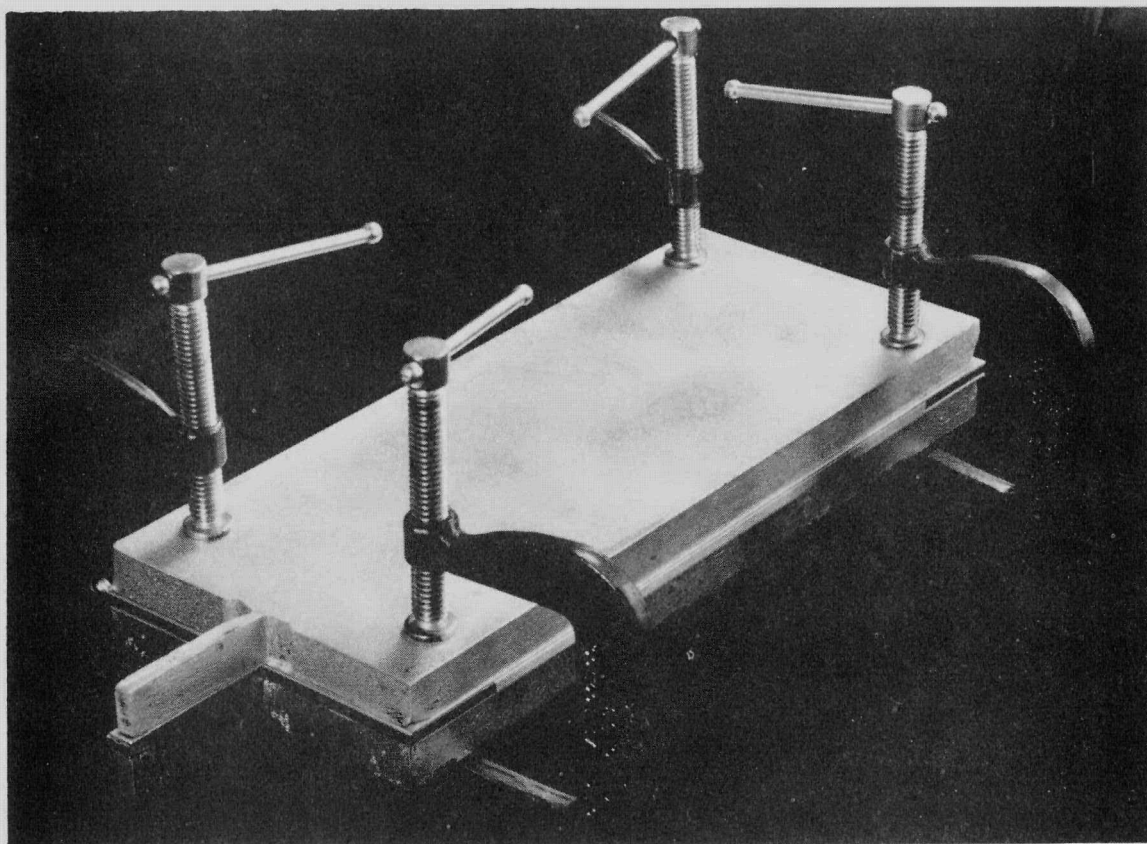
FIGURE 29. STEPS IN THE ASSEMBLY OF A TYPICAL ELEMENT FOR GAS-PRESSURE BONDING



1/2X

N64737

c. Completed Assembly of the Piece-Component Picture Frame Containing Compartmented Uranium Dioxide Cores  
The top cladding plate and copper cooling block for welding were placed on top of this assembly, as shown below.



1/2X

d. Assembled Fuel Element Clamped Between Copper Cooling Blocks Ready to be Fusion Edge-Welded

FIGURE 29. (CONTINUED)

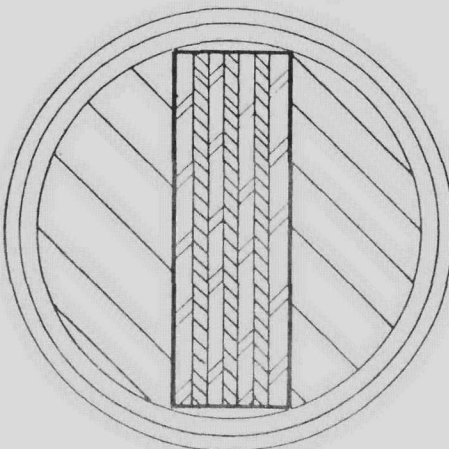
a gastight seal. Initially in this program, the edge-welded elements were sealed by induction melting the end of the evacuation extension while the entire element was contained in a vacuum chamber. This technique resulted in slight heating of the elements, however, and the resistance-upset welding method was used for all later specimens.

The assembled and sealed fuel plates were loaded into an autoclave such as described in BMI-1374(2) in detail. In these studies, it was found that the edge-welded elements should be loaded into the autoclave by a technique utilizing a loading tube in order to avoid warpage of the elements and contamination of the cladding during the bonding operation.

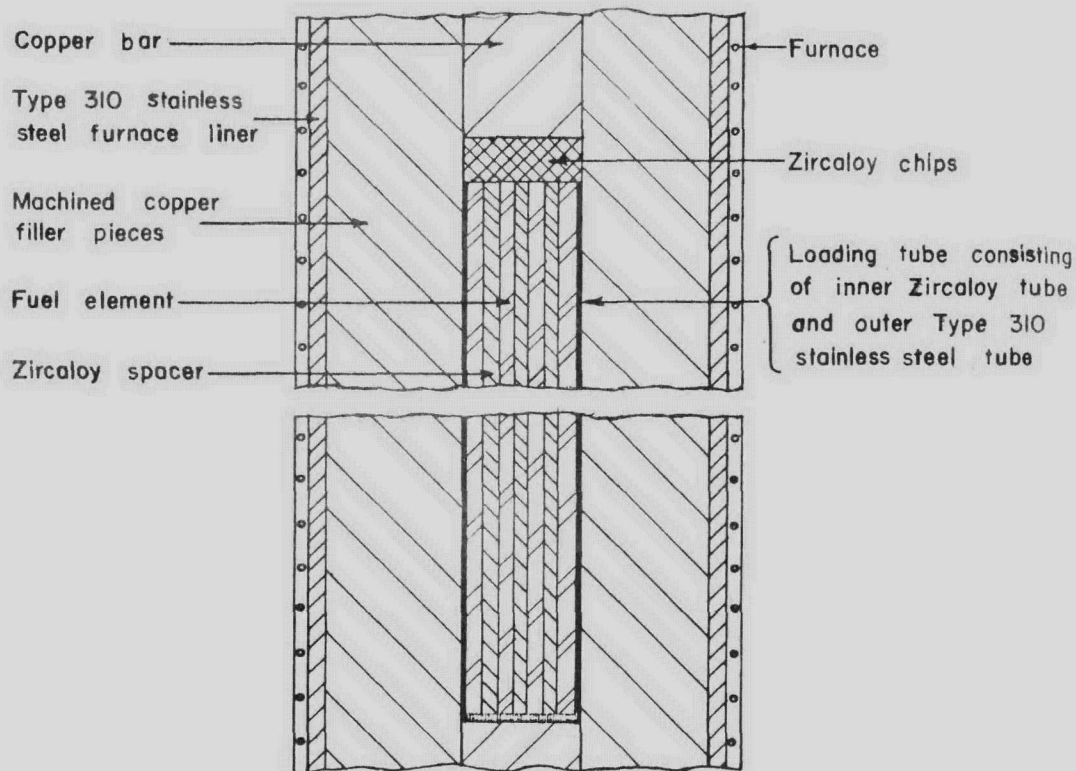
The loading procedure employed in this program is illustrated in Figure 30. For this procedure, a rectangular Zircaloy loading tube is constructed to very close tolerances and a structural Type 310 stainless steel container is then fit tightly around the Zircaloy tube to provide strength at the bonding temperature. This composite loading tube, closed at the bottom, will accommodate four elements. The elements are separated by Zircaloy spacers which are packed into the loading tube for each run. When more than four elements were to be run, the additional ones were placed in a loading tube vertically above the original tube, since the hot zone of the autoclave furnace was of sufficient length to accommodate the two loading tubes. Zircaloy chips and shimming stock were placed in the top of the loading tube to help purify the atmosphere. Two half cylinders of copper were machined to fill all void space in the inside of the cylindrical autoclave furnace except for a 1-in. -thick slot in the center into which the loading tube containing the elements was placed. Pieces of copper bar were used to fill the remaining void space in the slot. The copper served to minimize temperature gradients in the furnace.

Pressure bonding was performed at 1525 or 1550 F for 4 hr using a helium pressure of 10,000 psi. Fuel elements containing chromium-coated cores were bonded at 1525 F, which is below the zirconium-chromium eutectoid temperature, in order to minimize diffusion of the chromium barrier into the Zircaloy cladding. Since a number of elements with the three types of core coatings were usually bonded at the same time in the autoclave, most of the elements in the program were bonded at 1525 F. When elements having only graphite-coated or crystalline-carbon-coated cores were bonded, a temperature of 1550 F was employed. During the pressure-bonding cycle, both the temperature and pressure were increased simultaneously. Usually, the specified operating temperature of 1525 to 1550 F and pressure of 10,000 psi were attained in about 1 hr, and these conditions were then maintained for the specified time of 4 hr. Helium gas was used for the pressure bonding; however, other inert gases, such as argon, can also be used.

The surfaces of the fuel elements after pressure bonding were cleaned by vapor blasting and then pickling in a hydrofluoric acid solution to remove any surface staining prior to heat treating or corrosion testing. Zircaloy surfaces treated in this manner exhibited excellent corrosion resistance.



(a) Cross Section of Autoclave Loading Assembly



(b) Longitudinal Section of Autoclave Loading Assembly

A-31520

FIGURE 30. SECTIONAL DRAWINGS OF AUTOCLAVE LOADING ASSEMBLY  
USED FOR GAS-PRESSURE BONDING EDGE-WELDED  
ELEMENTS

CONCLUSIONS

The gas-pressure-bonding technique has been established as a feasible method for preparing Zircaloy-clad flat-plate fuel elements containing compartmentalized uranium dioxide fuel. Fuel elements prepared during this program by the procedures developed behaved well in corrosion tests with purposely defected compartments, had consistently strong Zircaloy-to-Zircaloy bonds, possessed complete compartment integrity, revealed good dimensional control, and demonstrated strong, ductile cladding. A solid-state bond is achieved between all of the mating Zircaloy components but the UO<sub>2</sub> cores are not crushed, since only a minimum amount of deformation of the cladding components occurs to bring their surfaces into intimate contact for bonding.

It has been found in a previously reported study(2) that an additional 5-min heat treatment in an 1850 F salt bath subsequent to pressure bonding is not required when the elements are properly prepared prior to assembly for bonding.

Techniques which are suitable for production have been developed for applying crystalline-carbon coatings to the uranium dioxide cores by a pyrolytic process and for applying chromium coatings to the cores by vacuum evaporation to serve as barrier layers to prevent core-to-cladding reaction during pressure bonding. Crystalline carbon coatings 15 to 40  $\mu$ in. thick and vapor-deposited coatings of chromium 25 to 40  $\mu$ in. thick minimized core-to-cladding reaction during bonding.

A study was conducted of the flow of the cladding-plate material during pressure bonding into void spaces in the picture-frame assembly, since it had been found in a previous program(2) that excessive flow could result in severe localized depressions and thinning of the cladding. It has been determined in this present study that this effect of flow can be satisfactorily minimized by individually compartmentalizing the cores with Zircaloy ribs. This design also offers maximum restriction of any cladding failure occurring during service of the fuel element. Since the versatility of the gas-pressure-bonding technique permits the use of a Zircaloy picture frame assembled from strip components, the uranium dioxide cores can easily be separated into individual compartments by placing Zircaloy ribs between each of them. By studying the effect of flow of the cladding into intentional void spaces of various shapes and sizes in the picture-frame assembly of the fuel elements, the maximum amount of void space which can be tolerated without resulting in excessive flow has been determined for fuel elements having individually compartmentalized cores.

The process which has been developed and established as feasible for gas-pressure bonding these fuel elements consists, therefore, of using belt-abraded piece Zircaloy components to form the compartmented picture frame, inserting uranium dioxide cores with coatings of pyrolytic crystalline carbon or vacuum-evaporated chromium into the compartments, and fusion welding the edge of the picture frame and cladding plates. The fuel elements are then evacuated and sealed, loaded into a high-pressure autoclave by a developed procedure, and gas-pressure bonded at 1525 or 1550 F at 10,000 psi for 4 hr.

ACKNOWLEDGMENT

This work was sponsored by the Bettis Atomic Power Division of Westinghouse Electric Corporation. The authors are grateful to Dr. B. Lustman and Mr. E. Losco of Bettis for their cooperation and assistance during the course of this research.

REFERENCES

- (1) Paprocki, S. J., Hodge, E. S., and Carmichael, D. C., "Pressure Bonding of Zircaloy-Clad Flat-Plate Uranium Dioxide Fuel Elements", Nuclear Metallurgy, 5, 25-28 (October 29, 1958).
- (2) Paprocki, S. J., Hodge, E. S., Carmichael, D. C., and Gripshover, P. J., "Gas-Pressure Bonding of Zircaloy-Clad Flat-Plate Uranium Dioxide Fuel Elements", BMI-1374 (August 28, 1959).
- (3) "Pressurized Water Reactor (PWR) Project Technical Progress Report for the Period August 24, 1956, to October 23, 1956", WAPD-MRP-64 (October 23, 1956).
- (4) "Pressurized Water Reactor (PWR) Project Technical Progress Report for the Period October 24, 1956, to December 23, 1956", WAPD-MRP-65 (December 23, 1956).
- (5) "Pressurized Water Reactor (PWR) Project Technical Progress Report for the Period February 24, 1957, to April 23, 1957", WAPD-MRP-67 (April 23, 1957).
- (6) Mallett, M. S., Gerds, A. F., Lemmon, A. W., and Chase, D. L., "The Kinetics of the Zirconium-Uranium Dioxide Reaction", BMI-1028 (August 15, 1957).
- (7) Grisdale, R. O., Pfister, A. C., and Van Roosbroeck, W., "Pyrolytic Film Resistors: Carbon and Boro-Carbon", Bell Tech. J., 30, 271-314 (April, 1951).
- (8) Tolansky, S., Multiple Beam Interferometry of Surfaces and Films, Oxford, Clarendon Press (1948).
- (9) Paprocki, S. J., Hodge, E. S., Boyer, C. B., and Getz, R. W., "Gas-Pressure Bonding of Flat-Plate Fuel Assemblies", BMI-1312 (January 20, 1959).

SJP:ESH:EHL:EGW:PGJ:DCC/dnb